Massachusetts Institute of Technology
Department of Civil Engineering
Constructed Facilities Division
Cambridge, Massachusetts 02139

DYNAMIC STIFFNESS OF RECTANGULAR FOUNDATIONS

by

JOSE DOMINGUEZ

Supervised by

José M. Roesset

August 1978

Sponsored by the National Science Foundation
Division of Advanced Environmental Research
and Technology
NSF-RANN Grant No. ENV 77-18339

Research Report R78-20 Order No. 626

BIBLIOGRAPHIC DATA SHEET	1. Report No. MIT-CE-R78-20	2.	3. Recipient's Accession No. PB 131

4. Title and Subtitle

DYNAMIC STIFFNESS OF RECTANGULAR FOUNDATIONS

5. Report Date: August 1978

6.

7. Author(s): JOSE DOMINGUEZ; supervised by Jose M. Roesset

8. Performing Organization Rept. No. R78-20

9. Performing Organization Name and Address

Massachusetts Institute of Technology
Dept. of Civil Engineering
77 Massachusetts Avenue
Cambridge, MA 02139

10. Project/Task/Work Unit No.

11. Contract/Grant No.: NSF RANN ENV 77-18339

12. Sponsoring Organization Name and Address

National Science Foundation
1800 "G" Street, N.W.
Washington, D.C. 20550

13. Type of Report & Period Covered: Research 1978

14.

15. Supplementary Notes

This is the 1st report in a series under this grant.

16. Abstracts

The Boundary Element Method is used to determine the dynamic stiffnesses of rectangular foundations resting upon or embedded within an elastic half-space. The effects of mesh size and relaxed versus nonrelaxed boundary conditions are investigated for square surface foundations. The static stiffnesses and the frequency dependent stiffness coefficients are then obtained as a function of the aspect ratio for rectangular foundations. Solutions for embedded foundations are obtained and results showing the effects of the embedment ratio are presented.

17. Key Words and Document Analysis. 17a. Descriptors

soil-structure interaction
earthquake engineering
boundary element method
machine foundations
finite element modeling
seismic analysis

17b. Identifiers/Open-Ended Terms

17c. COSATI Field/Group 13 02 ; 8 13

18. Availability Statement

Release unlimited

19. Security Class (This Report) UNCLASSIFIED

20. Security Class (This Page) UNCLASSIFIED

Pages

22. Price

FORM NTIS-35 (REV. 3-72)

THIS FORM MAY BE REPRODUCED

USCOMM-DC 14952-P72

ABSTRACT

The Boundary Element method is applied to the determination of the dynamic stiffnesses of rectangular foundations resting on the surface of or embedded in an elastic half space. The procedure is applied first to surface square foundations, and the effects of mesh size and relaxed versus nonrelaxed boundary conditions (smooth versus rough footing) are investigated by comparing the results to other published solutions. It is found that the solution for the smooth footing, which is considerably more economical, is almost identical for practical purposes to that of a rough foundation. The static stiffnesses and the frequency-dependent stiffness coefficients are then obtained as a function of the aspect ratio for rectangular foundations.

Solutions for embedded foundations are again obtained using complex coupling between horizontal and vertical forces (and displacements) and through a simplified procedure based on relaxed boundary conditions. The agreement between both approaches is very good, the second one being much less expensive computationally. The effect of embedment ratio on the static stiffnesses and the dynamic coefficients (frequency dependent) is presented for a square and a rectangular foundation with an aspect ratio of 2.

The Boundary Element method seems to provide an accurate and computationally feasible procedure to solve truly three-dimensional problems in soil-structure interaction. The method has clear advantages over finite element solutions, particularly when dealing with a half-space and embedded foundations.

PREFACE

The work described in this report represents part of a research effort on Dynamic Soil Structure Interaction carried out at the Civil Engineering Department of M.I.T. under the sponsorship of the National Science Foundation, Division of Advanced Environmental Research and Technology, through Grant ENV 77-18339.

The work was conducted by Dr. José Dominguez, Assistant Professor at the Escuela Técnica Superior de Ingenieros Industriales, Madrid, Spain, who spent a year at M.I.T. under the auspices of a Fulbright grant. It was supervised by Professor José M. Roesset .

Table of Contents

Title Page	1
Abstract	2
Preface	3
Table of Contents	4
Chapter 1. Introduction	5
Chapter 2. Formulation	8
Chapter 3. Foundation Stiffnesses - Surface Foundations	17
Chapter 4. Embedded Foundations	33
Chapter 5. Conclusions and Recommendations.	57
References	59
Figures 1 and 2	16
Figures 3 - 16	21 - 32
Figures 17 -36.	37 - 56

Chapter 1

INTRODUCTION

The determination of the dynamic stiffnesses of surface and embedded foundations of different shapes consitutes an important part of soil-structure interaction analyses using the substructure method, and is also an interesting problem on its own for the design of machine foundations. Analytical solutions have been developed only for particular cases [20]. To take into account the effect of embedment and different shapes and because of the high cost of three-dimensional finite element models, several other approximate methods have been suggested. The methods that can deal with foundations of arbitrary shape are based on a fundamental solution corresponding to the behavior of the soil under a concentrated load.

For the static case, a solution for the stresses and displacements in an elastic half-space due to a point force in the interior was developed by Mindlin [15]. However, there is not an explicit analytical solution for the dynamic problem. Lambe [14] obtained Green's function for the response of an elastic half-space to a point load on the surface, but the solution is left in terms of an integral that is not always easy to evaluate and which requires an approximate numerical solution. Some of the approaches suggested to compute the dynamic stiffnesses of surface foundations of arbitrary shape are based on this solution.

Wong [22] and Wong and Luco [23] computed the dynamic compliances of a surface rigid massless foundation of arbitrary shape resting on an isotropic elastic half-space by dividing the soil-foundation interface into rectangular elements. The tractions were considered uniformly distributed within the elements. An expression for the displacement at the center of the elements was obtained adding the integrals of the product of the Green's function and the traction over each element. For the usual case of known displacements, what would be an integral equation was then transformed into a system of linear algebraic equations relating displacements at the center of the elements and tractions. The diagonal influence functions of this system were derived by Thomson and Kobori [18], and Wong [22] obtained the off-diagonal terms in a similar way. The solution involves a double integral

that has to be computed by a numerical procedure, and the presence of a single pole has to be taken into account [22]. Further applications on the dynamic behavior of surface foundations using this method have been reported by Werner et al. [21] and Wong and Luco [24].

Previous to the work by Wong and Luco, a similar method was used by Elorduy, Nieto and Szekeley [5], where tractions over each element were represented by a concentrated load at the midpoint. This approach was formulated for the vertical component and has the difficulty of producing a singularity in the displacement under the load. The problem was solved by shifting the observation point from the center of the element. This, however, has an important influence over the diagonal terms of the system of equations,and a large number of elements are necessary to obtain good results.

Kitamura and Sakurai[13] presented an approach similar to the previous ones, assuming a concentrated load on each element except to evaluate the displacement of the loaded element where a uniformly distributed load is considered in order to avoid the singularity. They computed the vertical and rocking stiffnesses of frictionless surface foundations considering the vertical component to be independent of the other two. The main difference in this method is that instead of using the Green's functions derived by Lambe [14], which imply an integral, an explicit and simpler approximate formula proposed by Tajimi was adopted. However, Tajimi's formula is only accurate for low values of $\omega \cdot \gamma / C_s$ (C_s = shear wave velocity of the soil) and consequently the method produces good results for low values of $\omega \cdot B / C_s$. (B = characteristic dimension of the foundation).

Numerical approaches have also been applied to solve the problem of the concentrated load on the half-space surface. Gazetas and Roesset [6] obtained the solution for a layered half-space by a harmonic decomposition of the load. Kausel [12] considered a layered stratum of finite depth and computed the response to the surface point load using a Finite Element model that includes consistent transmitting boundaries.

The surface point load permits only to work with surface foundations. For embedded foundations a more general fundamental solution is required.

Harkreider [8] presented the formulation for a buried concentrated load in a layered half-space. The motions and stresses are left in terms of integrals that have to be treated numerically. In the present work the dynamic stiffness of surface and embedded foundations are computed using the Boundary Element Method and considering the soil to be a linear elastic isotropic half-space. The fundamental solution is considered to be the response of the complete elastic region to a concentrated load. As obtained by Cruse and Rizzo [2], this solution is written in an explicit form which makes the computation of stresses and displacements at any point straight-forward. The Boundary Element Method allows working with surface and embedded foundations of arbitrary shape. The use of the complete region fundamental solution instead of the half-space one makes it necessary in certain cases to discretize not only the soil foundation interface, but also the soil surface surrounding the foundation. This discretization is needed in the cases of embedded foundations or surface foundations "welded" to the soil, but not for surface foundations with relaxed boundary conditions as considered in most previous works.

Chapter 2

FORMULATION

The Boundary Element Method has been increasingly used for the solution of engineering problems in the last few years. It was formulated for potential problems by Jaswon and Ponter [9] and for elastostatic as well as for elastodynamic problems by Rizzo and Cruse [16, 2, 3]. Swedlow and Cruse applied it also to elasto-plastic flow [17]. In the following the elastostatic formulation will be summarized first due to its simplicity and the elastodynamic formulation will follow as an immediate consequence. The method basically consists in dividing the boundary of the region under consideration into small elements and establishing a relation between tractions (stresses) and displacements over these elements. Due to the fact that the interior of the region does not have to be discretized, the method is suitable for problems involving large regions and among these for soil problems.

The formulation is based on the Betti-Maxwell reciprocity relation. Consider a body Ω with a boundary S under a certain load condition σ_{ij}, ε_{ij}, u_i, t_i, b_i being the stress, strain, displacement, traction and body force components. Assuming a virtual state "$*$" on the same body, the following can be established.[1]

$$\int_S t_i u_i^* dS + \int_\Omega b_i u_i^* \, d\Omega = \int_S t_i^* u_i dS + \int_\Omega b_i^* \, u_i \, d\Omega$$

Let the virtual state be the fundamental solution state produced for Kelvin's problem of a unit point load applied at a point P of the body supposed to be part of the infinite region (Fig. 1). The displacement at any point when the load is applied in the j direction is given by:

$$u_i^* = \frac{1}{16\pi G(1-\nu)r} \cdot \left\{(3-4\nu)\delta_{ij} + \frac{\partial r}{\partial x_i} \frac{\partial r}{\partial x_j}\right\} e_j \, .$$

[1] Tensor notation is used, a summation being implied when indices are repeated. The comma - index indicates partial differentiation with respect to the independent variable of the index.

In this expression r is the distance from the point P, e_j the unit vector in the direction of the load, G the shear modulus of the soil and δ_{ij} the Kronecker delta.

The tractions at a point on the surface with outer normal η are:

$$t_i^* = \frac{1}{8\pi(1-\nu)r^2} \left\{ \frac{\partial r}{\partial \eta} [(1-2\nu)\delta_{ij} + 3r_{,i}\, r_{,j}] + (1-2\nu)(\eta_j r_{,i} - \eta_i\, r_{,j}) \right\} \cdot e_j$$

For a problem with zero body forces, the previous equations can be written in the form $u_i^* = U_{ji}\, e_j$ and $t_i^* = T_{ji}\, e_j$. The basic relations become then

$$u_j^p = \int_S U_{ji}\, t_i\, dS - \int_S T_{ji}\, u_i\, dS$$

where u_j^p =displacement in direction j at point P.

This last equation is known as Somigliana's Identity and allows us to compute the displacement at any interior point from displacements and tractions over the boundary using the known functions U_{ji} and T_{ji}.

Somigliana's Identity can be established for any point P of the body but in order to establish a relation between prescribed and unknown boundary conditions the virtual load point P has to be taken at the boundary. This will lead to an integral equation of the first kind for a problem with specified displacements, to an integral equation of the second kind for known tractions and to a mixed formulation for a mixed boundary value problem.

When the point P is taken on the surface, the integrals along the boundary will present a singular point. The integration at the singularity can be done by isolating a small area S around P and doing single and double layer potential considerations or by the less rigorous but simpler argument used in referece [1].

It can be shown that

$$\lim_{\varepsilon \to o} \int_{S_\varepsilon} U_{ij}\, t_i \, dS = 0 \quad \text{and} \quad \lim_{\varepsilon \to o} \int_{S_\varepsilon} T_{ij}\, u_i \, dS = -\frac{1}{2} u_j^P$$

where ε = radius of the area S for a smooth boundary at the point P.

The Somigliana Identity can then be written for a boundary point.

$$\frac{1}{2} u_j^P = \int_S U_{ji}\, t_i \, dS - \int_S T_{ji}\, u_i \, dS$$

In a more general form:

$$C^P u_j^P = \int_S U_{ji}\, t_i \, dS - \int_S T_{ji}\, u_i \, dS \, .$$

Using matrix notation,

$$C^P u^P + \int_S T\, u \, dS = \int_S U\, t \, dS$$

with $C^P = I \cdot C^P$.

For cases where the boundary is not smooth at P, the coefficient C^P will not be equal to 1/2. However, in the eventual formulation its computation does not present any problem.

Solution of an integral equation like the one above in a systematic way is only possible by numerical procedures. To do so the boundary S will be divided into elements. For simplicity the displacements and tractions will be considered to be constant throughout each element and associated with its center. Higher order elements with several nodes can also be used (Fig. 2). For the node K the basic equation can be established,

$$C_k U_k + \sum_{n=1}^{N} \left[\int_{S_n} T \, dS\right] u_n = \sum_{n=1}^{N} \left[\int_{S_n} U \, dS\right] t_n \, ,$$

N being the total number of boundary elements.

The integrals are carried out numerically over the surface S_n of the elements, being also functions of the nodal point K under consideration. Calling

$$H_{kn} = \int_{S_n} T \, dS \quad \text{and} \quad G_{kn} = \int_{S_n} U \, dS$$

for each node.

$$C_k\, u_k + H_{kn}\, u_n = G_{kn}\, t_n \ .$$

The system of equations for the N nodes can be expressed in the following form:

$$C\ \overline{u} + H^*\ \overline{u} = G\ \overline{t}$$

$\overline{u}$ and $\overline{t}$ are vectors with the three displacement and traction components of the N nodes.

H^* and G are $3N \times 3N$ square matrices obtained assembling the 3×3 matrices that relate every two elements.

Making

$$H_{kn} = H^*_{kn} \qquad \text{when } k \neq n$$
$$H_{kn} = H^*_{kn} + C_k \quad \text{when } k = n$$

the system of equations can be written in compact form:

$$H\ \overline{u} = G\ \overline{t} \ .$$

The previous system of equations establishes a relation between displacements and tractions over the boundary of the body under study. At every point of the boundary, one of these conditions is known and thus solving the system, the other can be obtained.

It should be pointed out that the matrix H is not symmetric and also that both G and H have most of their elements different from zero. In spite of these factors that make the computations longer than those of the Finite Element Method for the same number of unknowns, the Boundary Element Method is in many cases more efficient because of the much smaller number of unknowns due to the fact that only the boundary of the region under study has to be discretized.

For cases that include infinite or semi-infinite regions as soil problems do, the method is particularly suitable. In fact, for the infinite region case only the internal boundaries have to be discretized. The kernels of the boundary integrals satisfy the regularity conditions, meaning that the product of virtual tractions and actual displacements and vice-versa tend to zero at least as fast as $1/r^3$ when r increases to infinity.

As a result the integrals over the infinitely distant boundary are zero. For problems where a semi-infinite region is considered, only the plane boundary has to be discretized. This surface is already infinite, but taking into account only the elements of a zone surrounding the loaded area will produce good results since the integral kernels decrease rapidly.

DYNAMIC FORMULATION. The same considerations that have been applied to elastostatics can be extended to elastodynamic problems. The basic relation will be the reciprocity equation established between the Fourier Transforms of the actual and virtual states.

$$\int_S \hat{t}_i \, \hat{u}_i^* \, dS + \int_\Omega \hat{b}_i \, \hat{u}_i^* \, d\Omega = \int_S \hat{t}_i^* \, \hat{u}_i \, dS + \int_\Omega \hat{b}_i^* \, u_i \, d\Omega$$

The fundamental solution will be here the response of the infinite medium to a unit concentrated harmonic force at a point P. This solution following the works by Doyle [4], and Cruse and Rizzo [2] can be obtained from the equations of motion of linear isotropic elastic bodies and are of the form:

$$\hat{U}_{ji} = \frac{1}{\alpha \pi \rho c_s^2} \left\{ \psi \delta_{ji} - \chi \, r_{,i} \, r_{,j} \right\}$$

$$\hat{T}_{ji} = \frac{1}{\alpha \pi} \left\{ \left(\frac{d\psi}{dr} - \frac{1}{r} \chi \right) \left(\delta_{ij} \frac{\partial r}{\partial \eta} + r_{,i} \, \eta_j \right) - \right.$$

$$- \frac{2}{r} \chi \left(\eta_i \, r_{,j} - 2 r_{,i} \, r_{,j} \frac{\partial r}{\partial \eta} \right) - 2 \frac{d\chi}{dr} r_{,i} \, r_{,j} \frac{\partial r}{\partial \eta}$$

$$\left. + \left(\frac{c_p^2}{c_s^2} - 2 \right) \left(\frac{d\psi}{dr} - \frac{d\chi}{dr} - \frac{\alpha}{2r} \chi \right) r_{,j} \eta_i \right\}$$

Functions $\hat{U}_{ji}$ and $\hat{T}_{ji}$ are defined as previously by $\hat{u}_i^* = \hat{U}_{ji} \, e_j$ and $\hat{t}_i^* = \hat{T}_{ji} \, e_j$. In the above expressions α is an integer number equal to 2 for the two-dimensional case and to 4 for three dimensions. The functions χ and ψ for three dimensions are given by:

$$\chi = \left(-\frac{3\,C_s^2}{\omega^2 r^2} + \frac{3C_s}{i\omega r} + 1\right)\frac{e^{-\frac{i\omega r}{C_s}}}{r} - \left(\frac{C_s^2}{C_p^2}\right)\left(-\frac{3\,C_p^2}{\omega^2 r^2} + \frac{3C_p}{i\omega r} + 1\right)\frac{e^{-\frac{i\omega r}{C_p}}}{r}$$

$$\psi = \left(1 - \frac{C_s^2}{\omega^2 r^2} + \frac{C_s}{i\omega r}\right)\frac{e^{-\frac{i\omega r}{C_s}}}{r} - \left(\frac{C_s^2}{C_p^2}\right)\left(-\frac{C_p^2}{\omega^2 r^2} + \frac{C_p}{i\omega r}\right)\frac{e^{-\frac{i\omega r}{C_p}}}{r}$$

The obtained functions $\hat{U}_{ji}$ and $\hat{T}_{ji}$ also satisfy the same conditions at the boundary singularity as U_{ji} and T_{ji} for the static case. Following an equal pattern to the one described there the system of equations can be assembled:

$$H\,\overline{u} = G\,\overline{t}$$

The kernels of the integrals involved in the formulation satisfy also the regularity conditions for the dynamic case and consequently the boundaries at an infinite distance do not have to be taken into account.

For two dimensions the fundamental solution remains in the same form and χ and ψ are given in terms of the Bessel functions.

$$\chi = K_2\left(\frac{i\omega r}{C_s}\right) - \frac{C_s^2}{C_p^2}\,K_2\left(\frac{i\omega r}{C_p}\right)$$

$$\psi = K_o\left(\frac{i\omega r}{C_s}\right) + \frac{C_s}{i\omega r}\left[K_1\left(\frac{i\omega r}{C_s}\right) - \frac{C_s}{C_p}\,K_1\left(\frac{i\omega r}{C_p}\right)\right]$$

COMPUTER IMPLEMENTATION FOR FOUNDATION STIFFNESS. A program was written using the method described above to compute the stiffness of foundations of arbitrary shape, embedded, or on the surface of the soil considered as an elastic isotropic half-space. The foundation stiffnesses can be calculated considering the three components of the motion and traction to be coupled as established in the general formulation. However, it can be assumed that the vertical tractions and displacements are independent of those in the two horizontal directions and thus for surface foundations, vertical and rocking components of the stiffness are computed establishing a relation between vertical tractions and displacements only and the horizontal and torsional stiffnesses are computed considering both horizontal

components coupled. This assumption is consistent with that of relaxed boundary conditions used by other researchers when studying the stiffness of foundations by different methods. To compute the rocking stiffness for embedded foundations taking into account the previous assumption, one has to decompose the motion of the side walls into two parts: a motion that includes only the vertical component and a rotation of the side walls around the base that will produce horizontal displacements. Results using relaxed and non-relaxed boundary conditions will be compared in the following section.

For all the problems analyzed in the present work, rectangular boundary elements have been used. Tractions and displacements are constant throughout each element and associated with a nodal point at its center. The soil-foundation interface as well as the soil outside the foundation were modeled with rectangular elements that on the free surface increased in size as the distance to the foundation increased. Only a few free-field elements were, however, needed, since their influence on the foundation stiffness is small.

Consider the 3×3 element matrices H_{kn} and G_{kn} that relate the element k to the n, being $k \neq n$. Let

$$\Delta T_{ji} = \int_{S_n} T_{ji} \, dS$$

Then

$$H_{kn} = \left[\begin{array}{cc:c} \Delta T_{11} & \Delta T_{12} & \Delta T_{13} \\ \Delta T_{21} & \Delta T_{22} & \Delta T_{23} \\ \hdashline \Delta T_{31} & \Delta T_{32} & \Delta T_{33} \end{array}\right]$$

for two elements that belong to the same horizontal plane, only the terms ΔT_{13}, ΔT_{23}, ΔT_{31} and ΔT_{32} of the matrix H_{kn} are different from zero. When relaxed boundary conditions are assumed, only the upper left and lower right parts of the matrix are used, and since the tractions are zero for the free-field elements, both products $G_{kn}\ t_n$ and $H_{kn}\ u_n$ will be zero.

These elements will not have, therefore, any influence on the other elements on their own plane, and for surface foundations no elements are necessary on the free part of the soil surface.

One of the problems that requires attention in the implementation of the method is the integration of the fundamental solution over the elements to obtain the terms of the G and H matrices. When the integration has to be performed over an element different from the one where the virtual load is applied, it does not present any problem, and a normal numerical integration procedure can be applied. In the present work a nine point standard Gaussian quadrature method was used. The element matrices H_{nn} and K_{nn} require, however, a different treatment because of the integration around a singular point. For each type of rectangular element (displacement expansion), one can, however, estimate the value of the integrals from analytical considerations, once the singular point is excluded. In the computation of the integrals

$$\int_{S_n} T_{ij} \, dS$$

$$\int_{S_n} U_{ij} \, dS$$

For i = j a series expansion of the exponential function was used, and the integral was then computed analytically.

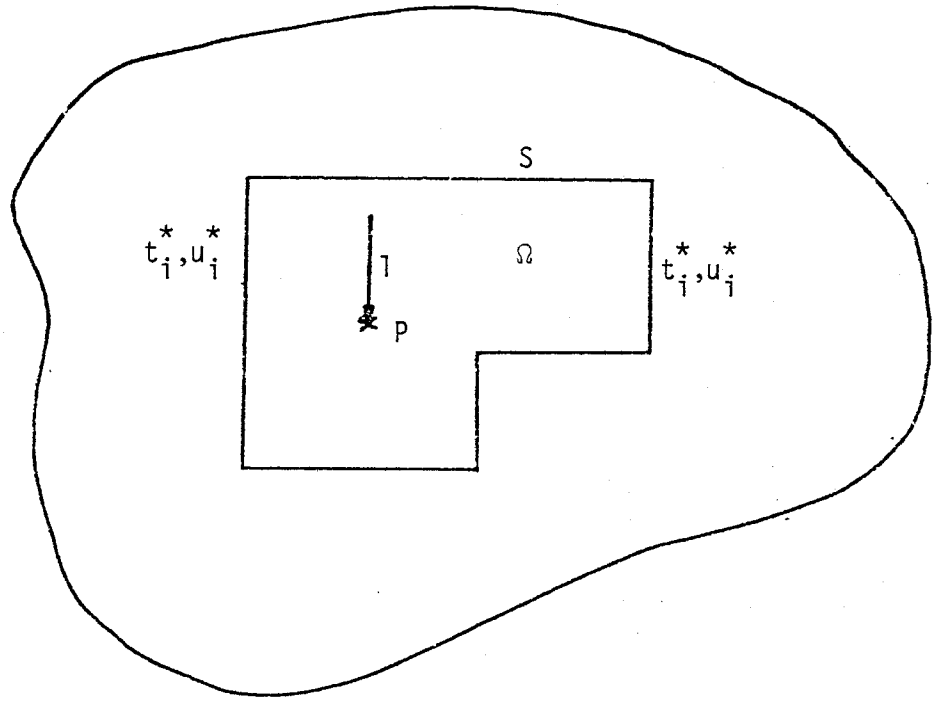

Figure 1 - Virtual State over the Body Ω

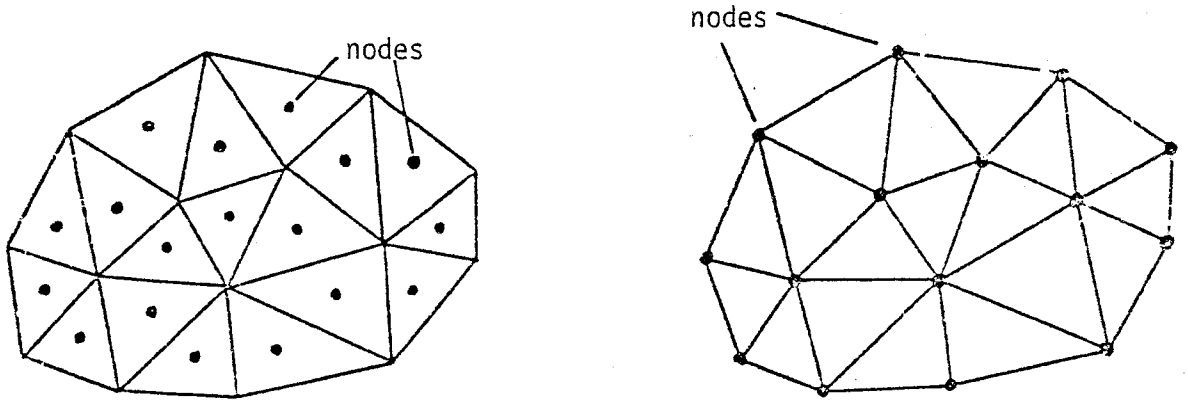

Figure 2 - Boundary Discretization for 3-D Problem

Chapter 3

FOUNDATION STIFFNESSES - SURFACE FOUNDATIONS

Using the procedure described in Chapter 2, parametric studies were conducted of the dynamic stiffness of square and rectangular foundations with different aspect ratios, resting on the surface or with different levels of embedment. Results were obtained considering relaxed and non-relaxed boundary conditions in several cases and also a comparison was performed with other published results for square and circular equivalent foundations. The dynamic formulation produces an indeterminate value for a zero frequency, and the static stiffnesses were computed using the results for a very low value of the frequency.

To study the variation of the stiffness components with frequency, they were expressed in the form

$$K_{ij} = \overset{\circ}{K}_{ij} \, (k_{ij} + i \, a_o \, C_{ij})$$

where $\overset{\circ}{K}_{ij}$ is the static value

k_{ij} and C_{ij} are frequency-dependent coefficients

$a_o = \omega \cdot B/C_s$ is a dimensionless frequency

B is the half-side for square foundations and half of the smallest side for rectangular footings

C_s is the shear wave velocity of the soil.

When an internal hysteretical damping is considered in the soil, the dynamic stiffness can be given by the approximate expression:

$$K_{ij} = \overset{\circ}{K}_{ij} \, (k_{ij} + i \, a_o \, C_{ij})(1 + 2iD),$$

where D is the damping ratio. In reality the coefficients k_{ij} and C_{ij} depend on D, but for typical values this dependence is small.

SURFACE FOUNDATIONS: A series of studies were first conducted in order to assess the accuracy of the method, and determining the dynamic stiffness of a surface square foundation. Results were obtained considering first re-

laxed boundary conditions, i.e., vertical direction independent of the other two, and subdividing the surface of the foundation into 3×3, 6×6 and 8×8 equal square elements. Figure 3 shows the model and the coordinate system. All the results obtained are for values of the shear modulus G=1 and Poisson's modulus ν=1/3.

Figure 4 shows a comparison of the vertical compliance obtained using two different meshes and the results published by Wong and Luco [23]. The results show a good agreement between the methods even for a model with only nine elements.

Following a procedure proposed by Kausel [12], the results obtained for different meshes were extrapolated. In this case, however, when using constant displacement square elements, the extrapolation law is not known a priori. Results were obtained for a certain frequency, and several meshes for square and rectangular foundations, and from them the extrapolation law was decided to be linear with the element size for the displacement components of the stiffness and quadratic for the rotations. In Table I results are compared for the static stiffness coefficients using relaxed and non-relaxed boundary conditions and also with results by J.J. Gonzalez [7] for surface square foundations. For our two cases the values are extrapolated linearly with the size of the elements under the foundation. In the non-relaxed boundary conditions case, the free field around the foundation was modeled with forty square elements increasing in size with distance to the foundation and covering a square surface the side of which was seven times the side of the foundation.

TABLE I - STATIC STIFFNESS FOR SQUARE FOUNDATIONS

	Relaxed B.C.	Non-relaxed B.C.	After J.J. Gonzalez
K°_{xx}/GB	5.679	5.61	5.52
K°_{zz}/GB	7.324	7.126	6.9
$K^{\circ}_{\phi_1\phi_1}/GB^3$	5.774	5.688	6.
$K^{\circ}_{\phi_3\phi_3}/GB^3$	7.528	7.479	8.2

Figures 5 to 8 show the variation with frequency of the stiffness coefficients. Results using both relaxed and non-relaxed boundary conditions are plotted. The agreement is good for the displacement components and excellent for the rotations. The non-relaxed boundary condition results present a decay in Figures 5 and 6 for the highest values of frequency represented. This is due to the fact that the elements in the free field are larger than the ones inside, and they are no longer appropriate to reproduce a motion with the wave length corresponding to this range of frequency. In Figures 5 and 7 the results are also compared to those computed using the values given by Veletsos and Wei [20] for circular foundations. An equivalent radius was computed for each stiffness component: the radius of a foundation with the same surface, i.e., $R = \sqrt{4/\pi}\ B$, for the vertical stiffness and the radius of a foundation with the same moment of inertia, i.e., $R = \sqrt[4]{16/3\pi}B$, for the rocking stiffness. It can be seen in Figures 5 and 7 that there is good agreement between the three solutions.

The variation of stiffness with the aspect ratio for surface rectangular foundations was also studied using the Boundary Element Method and assuming relaxed boundary conditions. The shortest half-side of the foundation, B, was set equal to 1 and the other took values from 1 to 4. Each foundation was studied using two meshes of square elements: one with three elements along the shortest side and the other with four. From these meshes the values of the stiffnesses were computed again by a linear extrapolation for displacement components and a quadratic extrapolation for the rotations. Figure 9 represents the variation of the static stiffness with A/B. It can be pointed out that the three displacement components and the rotation ϕ_1 follow almost a straight line and that could be used as an approximation. This figure also shows a comparison with results given by approximate formulae proposed by C. Vardanega. In Figure 10 the static stiffnesses are presented normalized by their own values for the square foundation.

The variation of the stiffness coefficients with the dimensionless frequency $a_o = \omega \cdot B/C_s$ and with the aspect ratio A/B are represented in the next figures. The terms K_{xx} and C_{xx} are shown in Figure 11. It can be noticed that these coefficients have very little variation with frequency and only C_{xx} has a shifting with A/B. The terms K_{yy} and C_{yy}, in Figure 12, present

more variation with both frequency and aspect ratio. When A/B grows, the variation versus a_o tends to be of the form of that for the strip footing, as could be expected. Figure 13 shows the variation for the vertical stiffness coefficients which has a similar shape to the variation for K_{xx} and C_{xx}. In this case, there is, however, more variation of the coefficients with respect to a_o and A/B and in particular the damping coefficient C_{zz} is always larger than C_{xx}.

Figure 14 shows the variation of the coefficients for rocking around the longest axes of the foundation. It is interesting to notice that there is no variation of $K_{\phi_1\phi_1}$ when A/B changes. The term $C_{\phi_1\phi_1}$ has negligible values in the low frequency range. It increases in value with frequency and varies only slightly with the aspect ratio A/B. The coefficients for rocking around the short axis are represented in Figure 15. The $K_{\phi_2\phi_2}$ coefficient presents some variation with respect to A/B from the square to the 2×1 foundation, but it does not change as much with the aspect ratio and for larger values of A/B it has some fluctuations with the increase in a_o. The damping term $C_{\phi_2\phi_2}$ grows much faster with A/B than the $C_{\phi_1\phi_1}$ term. Figure 16 shows the stiffness coefficients for the torsion around the vertical axes. The $K_{\phi_3\phi_3}$ term presents a similar variation with frequency for all the ratios A/B considered, but with more fluctuations as A/B increases. The variation with frequency and aspect ratio of $C_{\phi_3\phi_3}$ is also of the same shape as those of the other rotation damping terms, but while none of the others got to a stable value in the range a_o and A/B represented, this term reaches it for the higher values of those parameters.

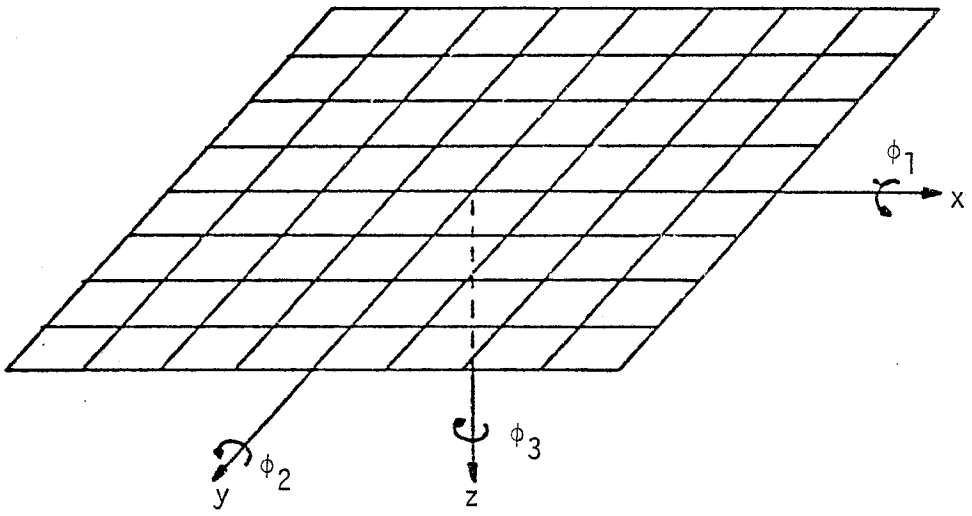

Figure 3 - 8 × 8 Elements Discretization and System of Coordinates

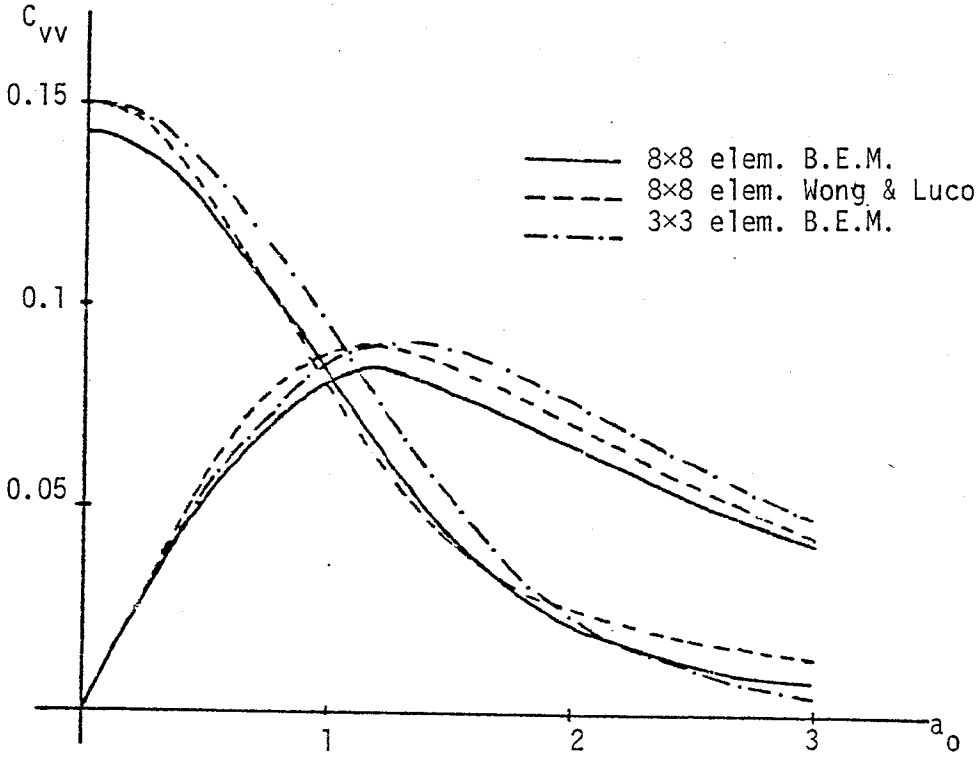

Figure 4 - Vertical Compliance for a Surface Square Foundation

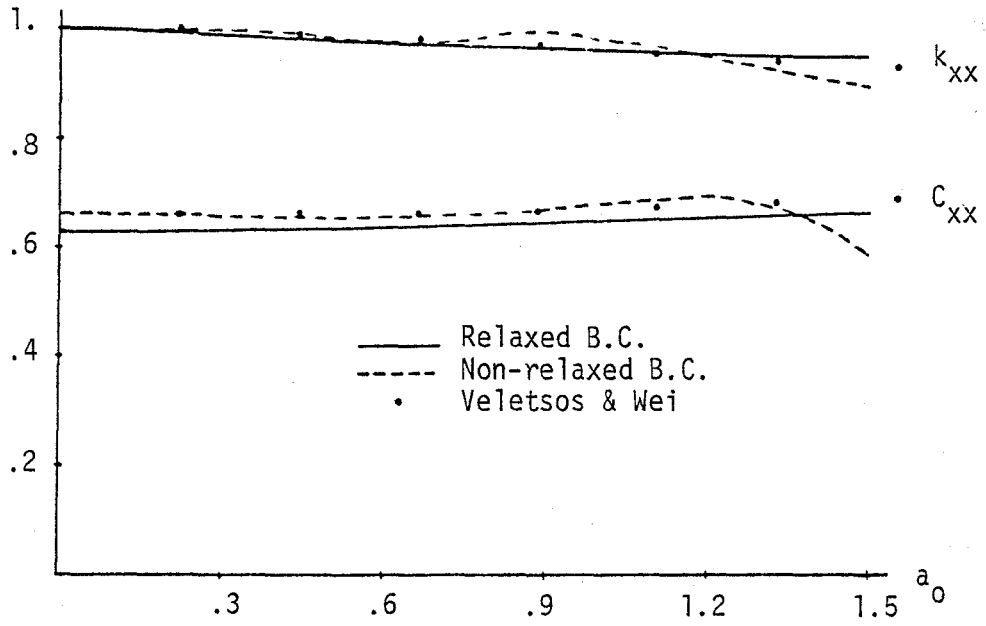

Figure 5 - Horizontal Stiffness Coefficients.
Square Foundation

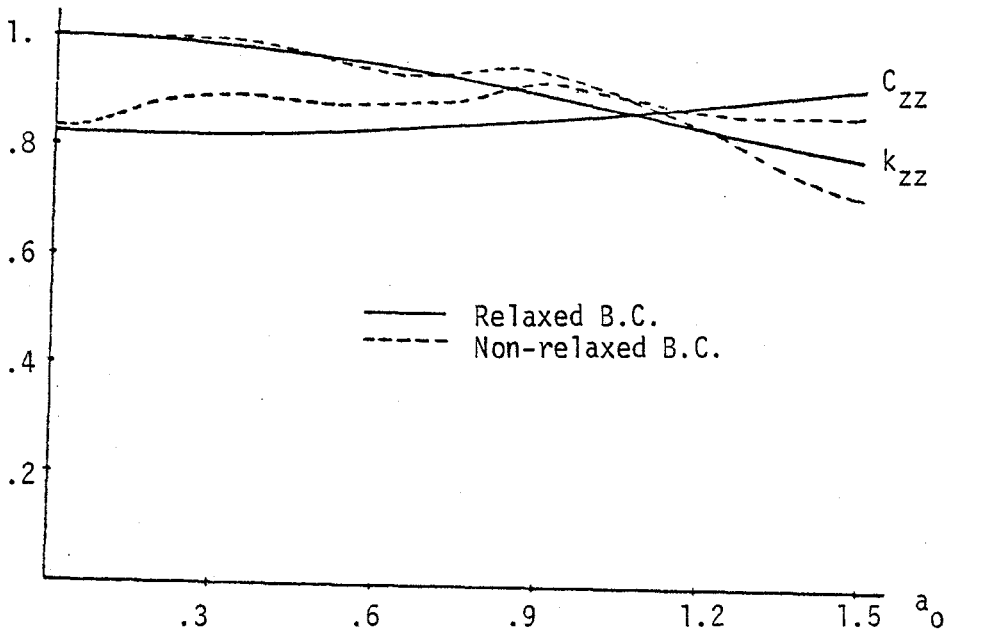

Figure 6 - Vertical Stiffness Coefficients.
Square Foundation

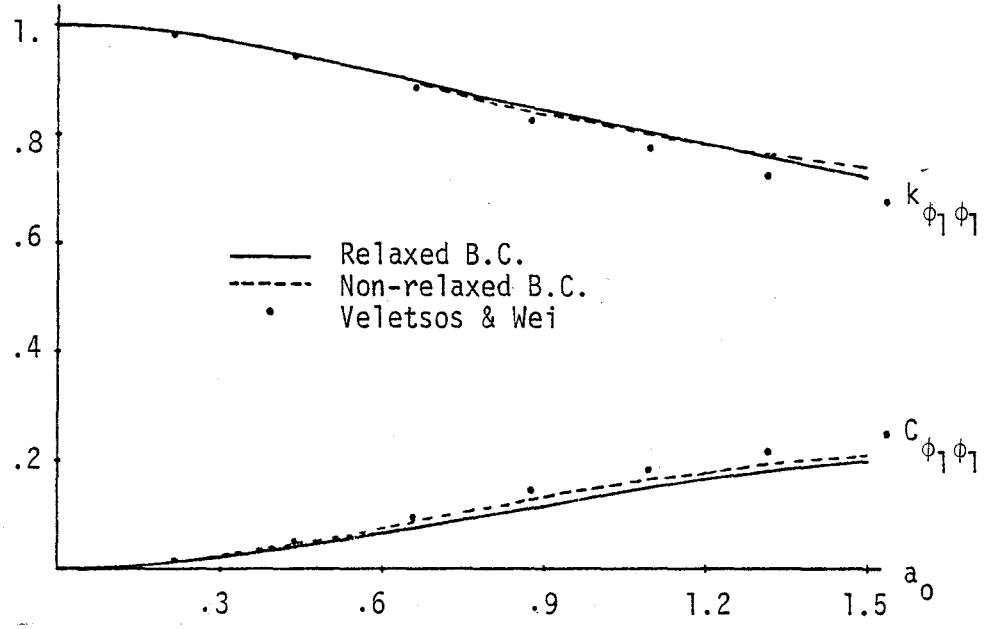

Figure 7 - Rocking Stiffness Coefficients.
Square Foundation.

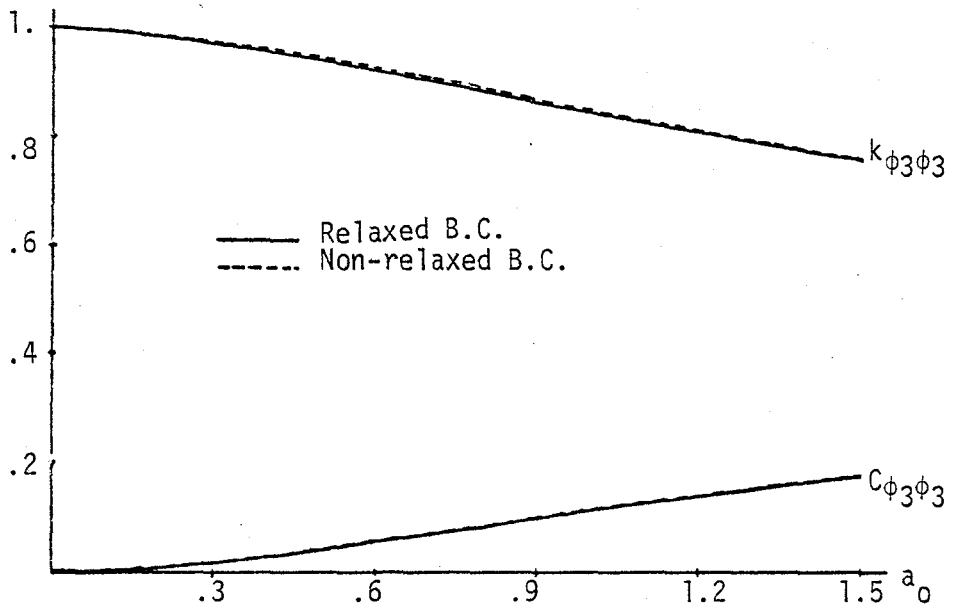

Figure 8 - Torsional Stiffness Coefficients.
Square Foundation.

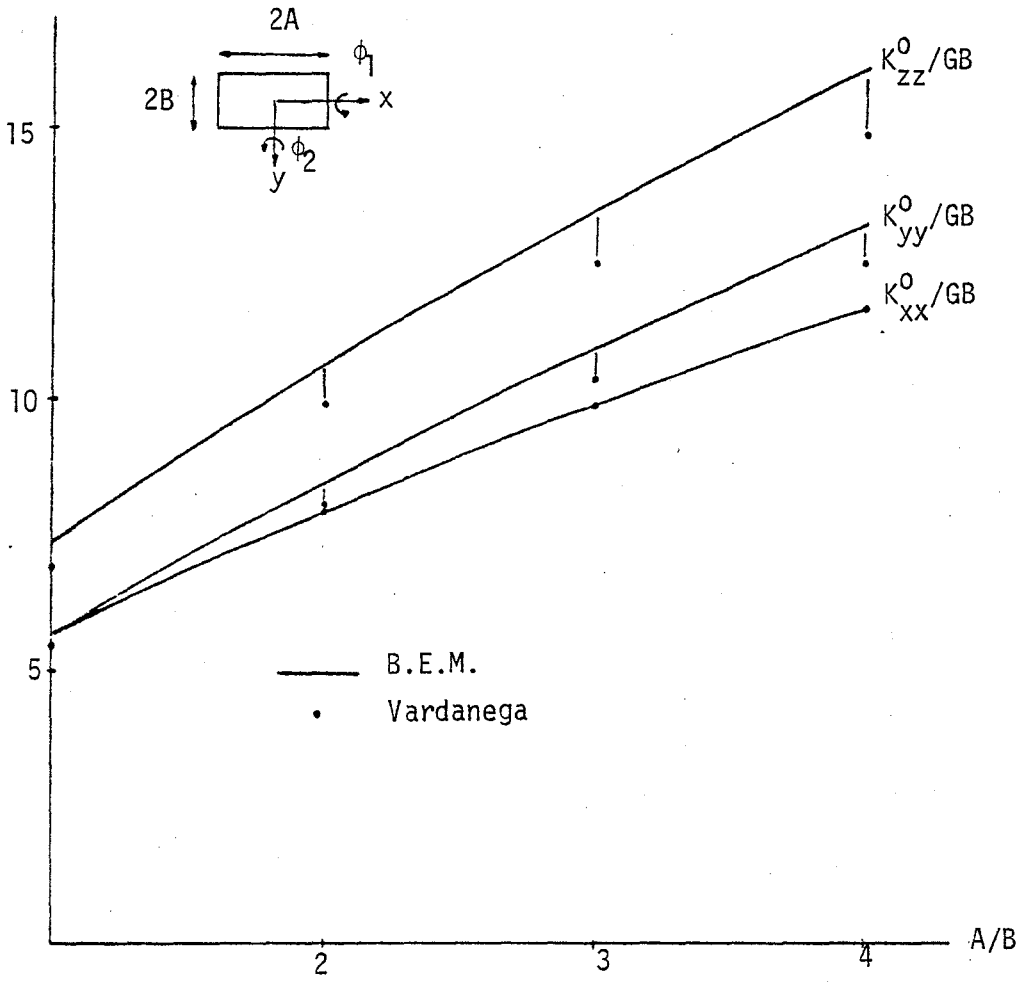

Figure 9a - Static Stiffness for Surface Rectangular Foundations. Displacements.

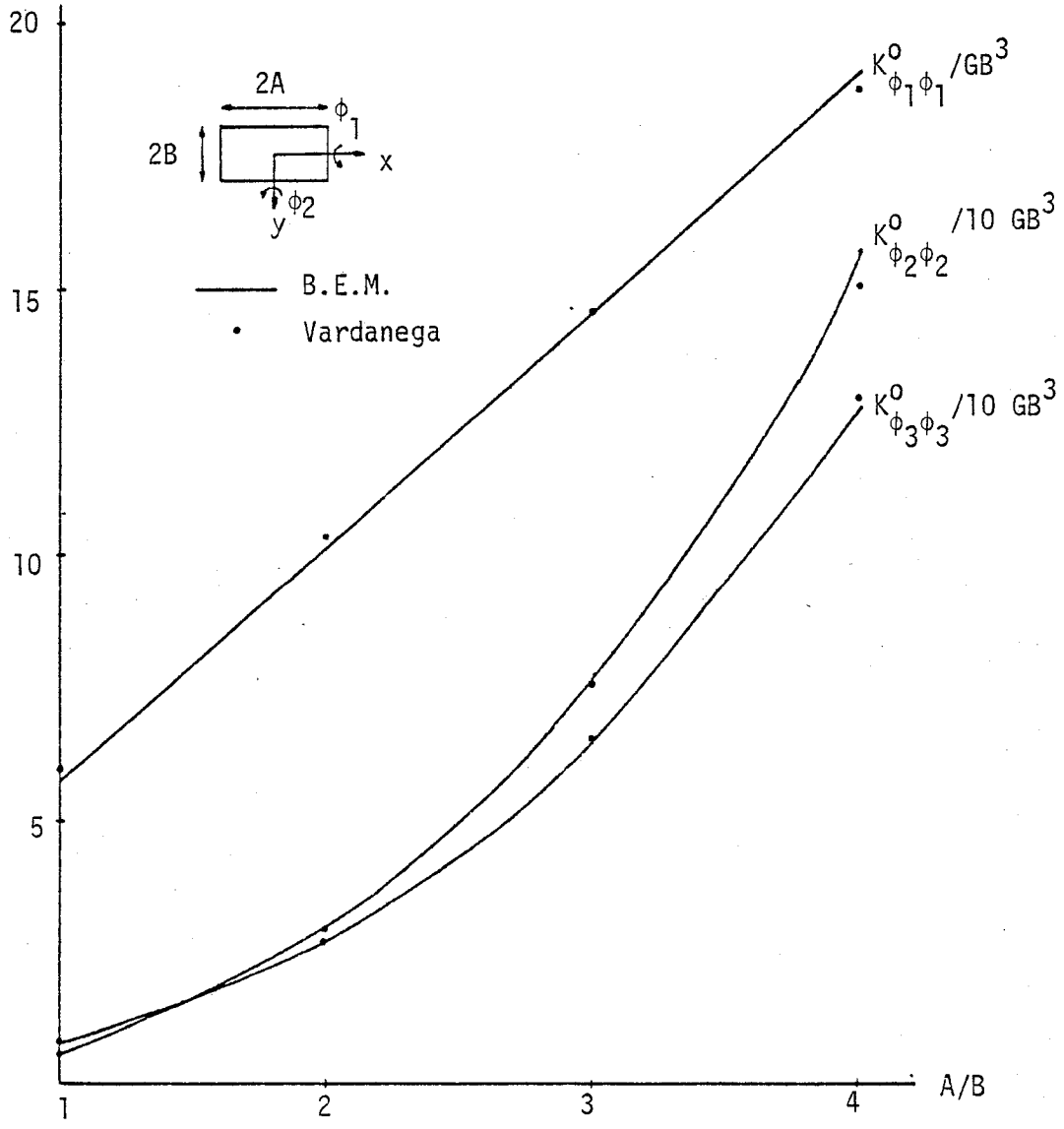

Figure 9b - Static Stiffness for Surface Rectangular Foundations. Rotations.

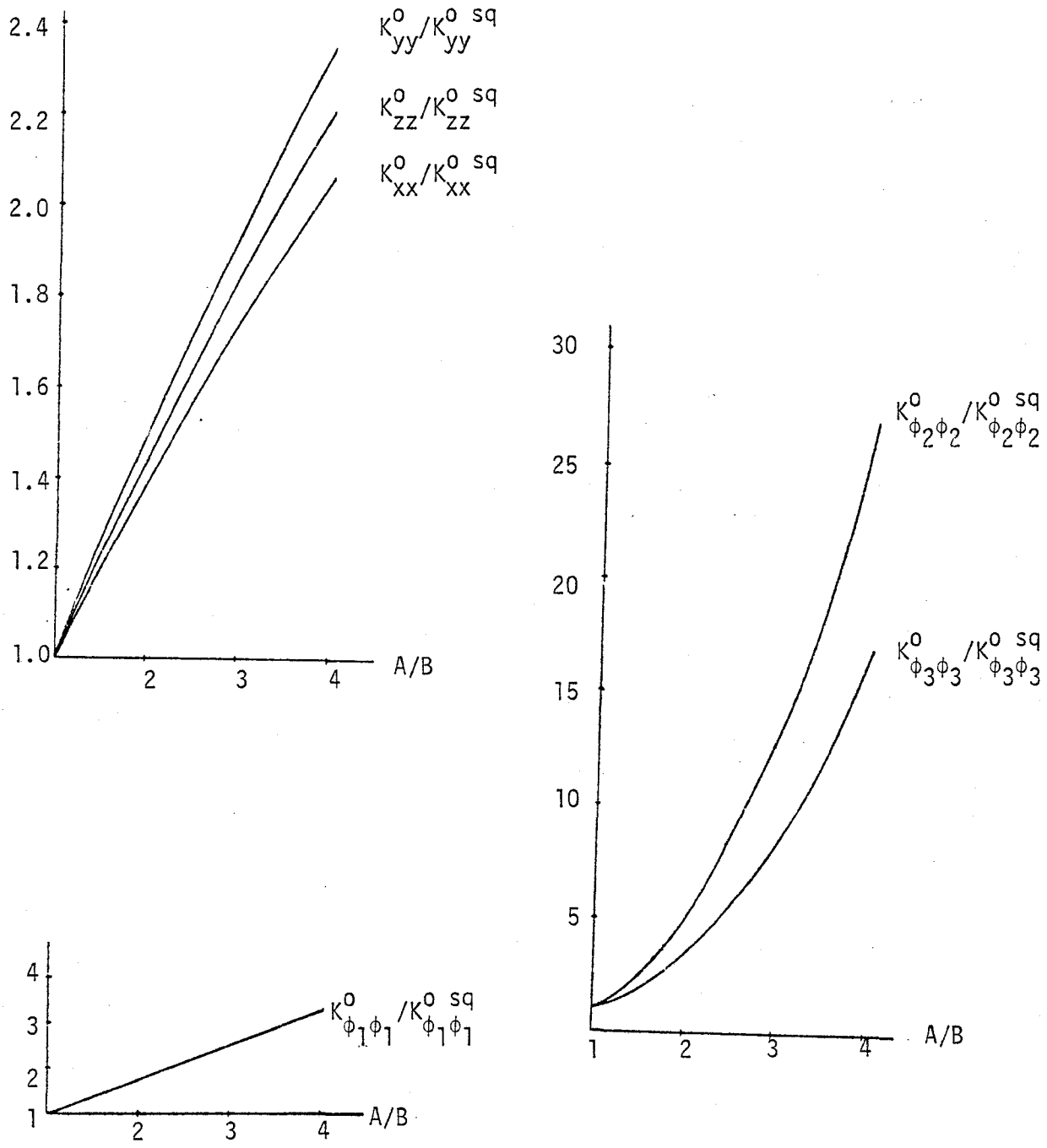

Figure 10 - Static Stiffness/Static Stiffness of Square Foundation.

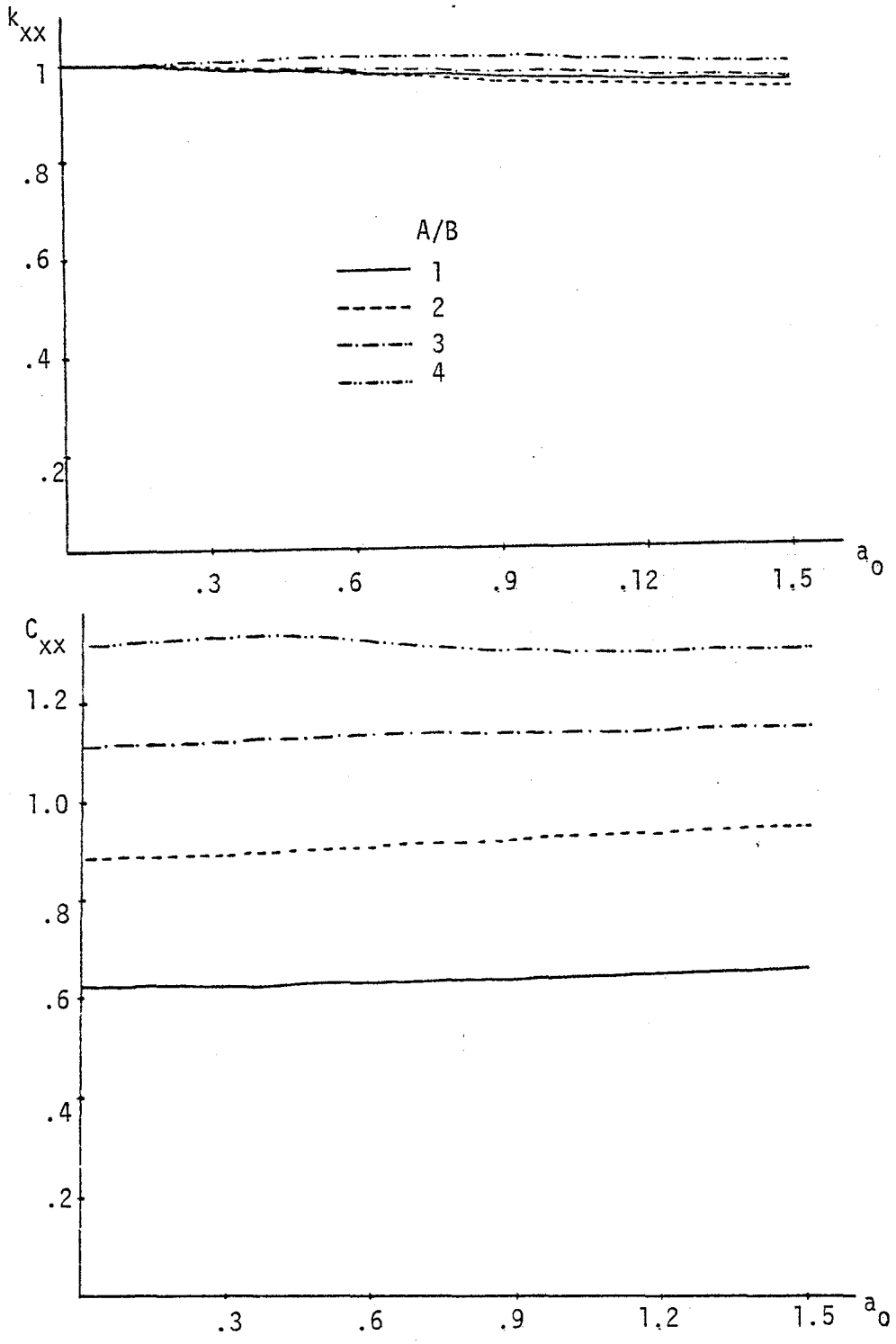

Figure 11 - Horizontal Stiffness Coefficients

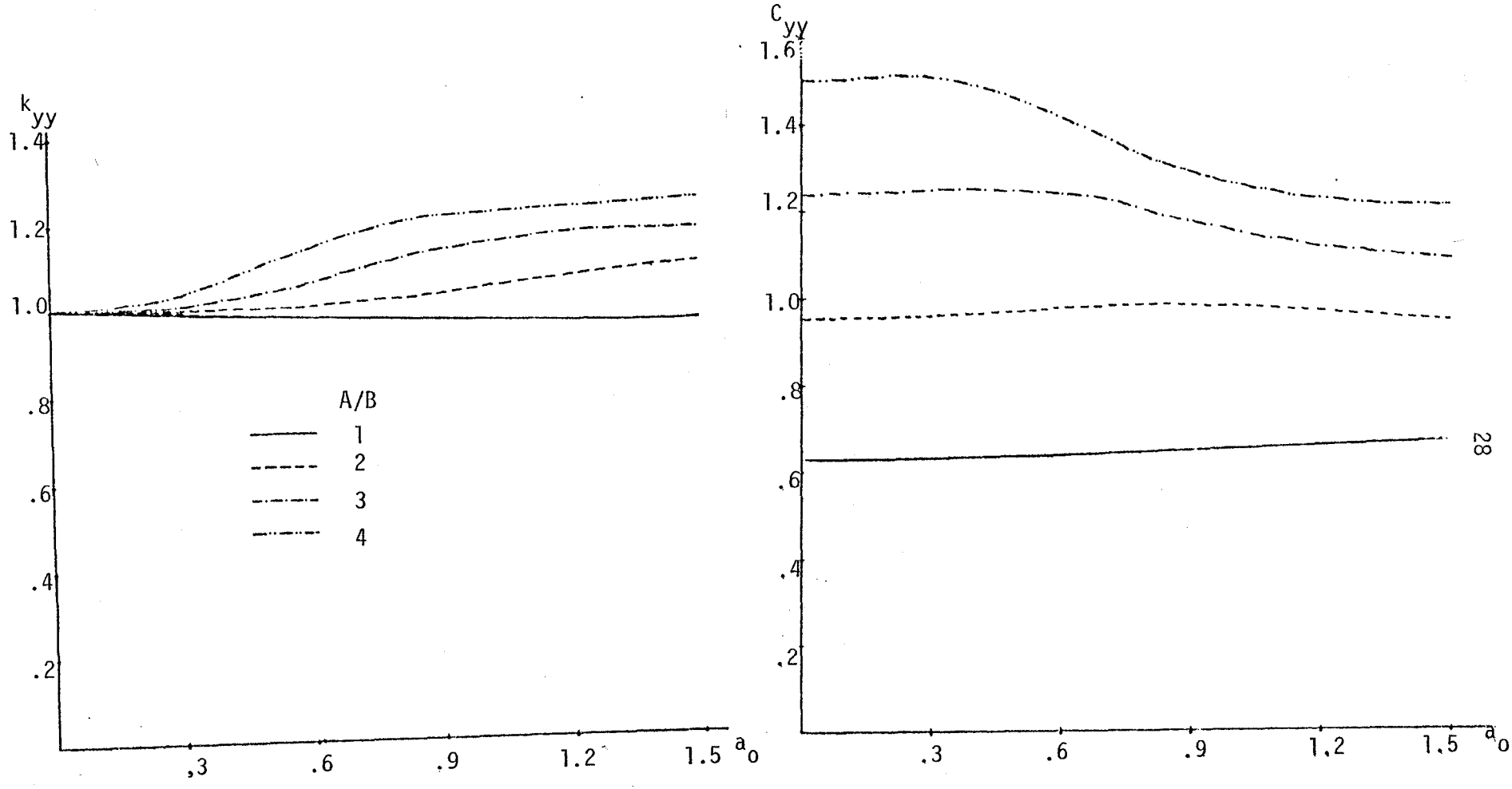

Figure 12 - Horizontal Stiffness Coefficients.

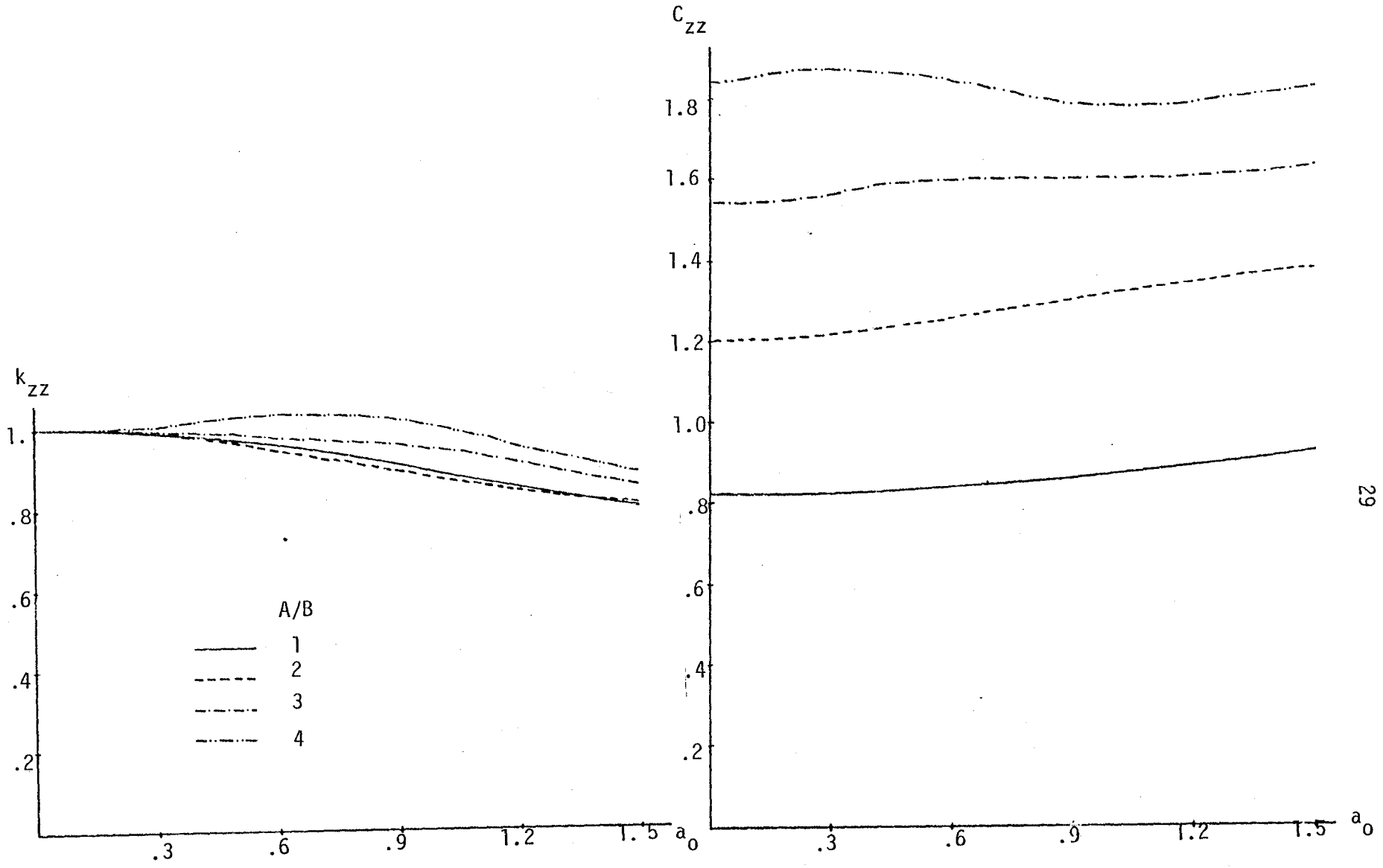

Figure 13 - Vertical Stiffness Coefficients

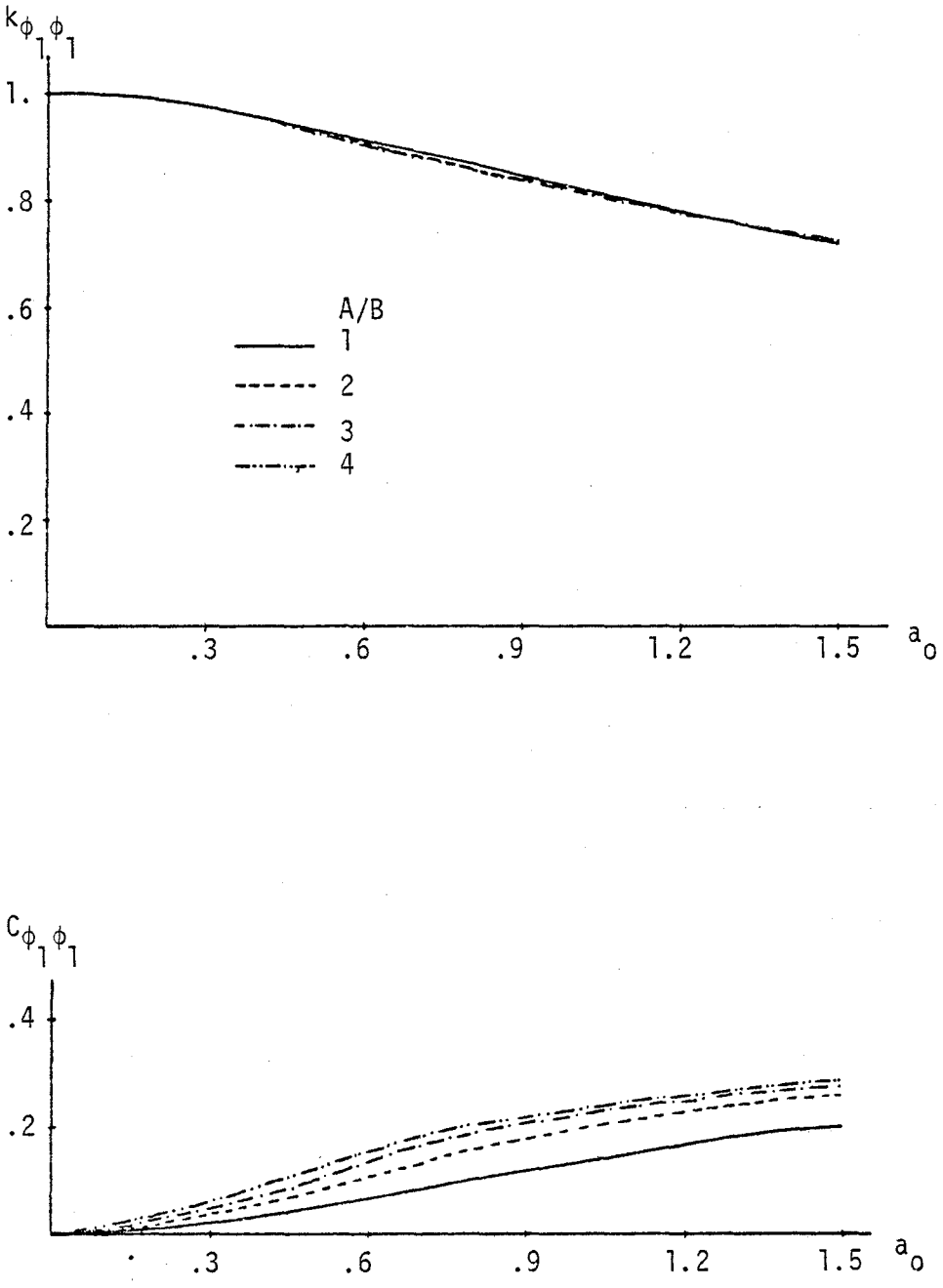

Figure 14 - Rocking Stiffness Coefficients

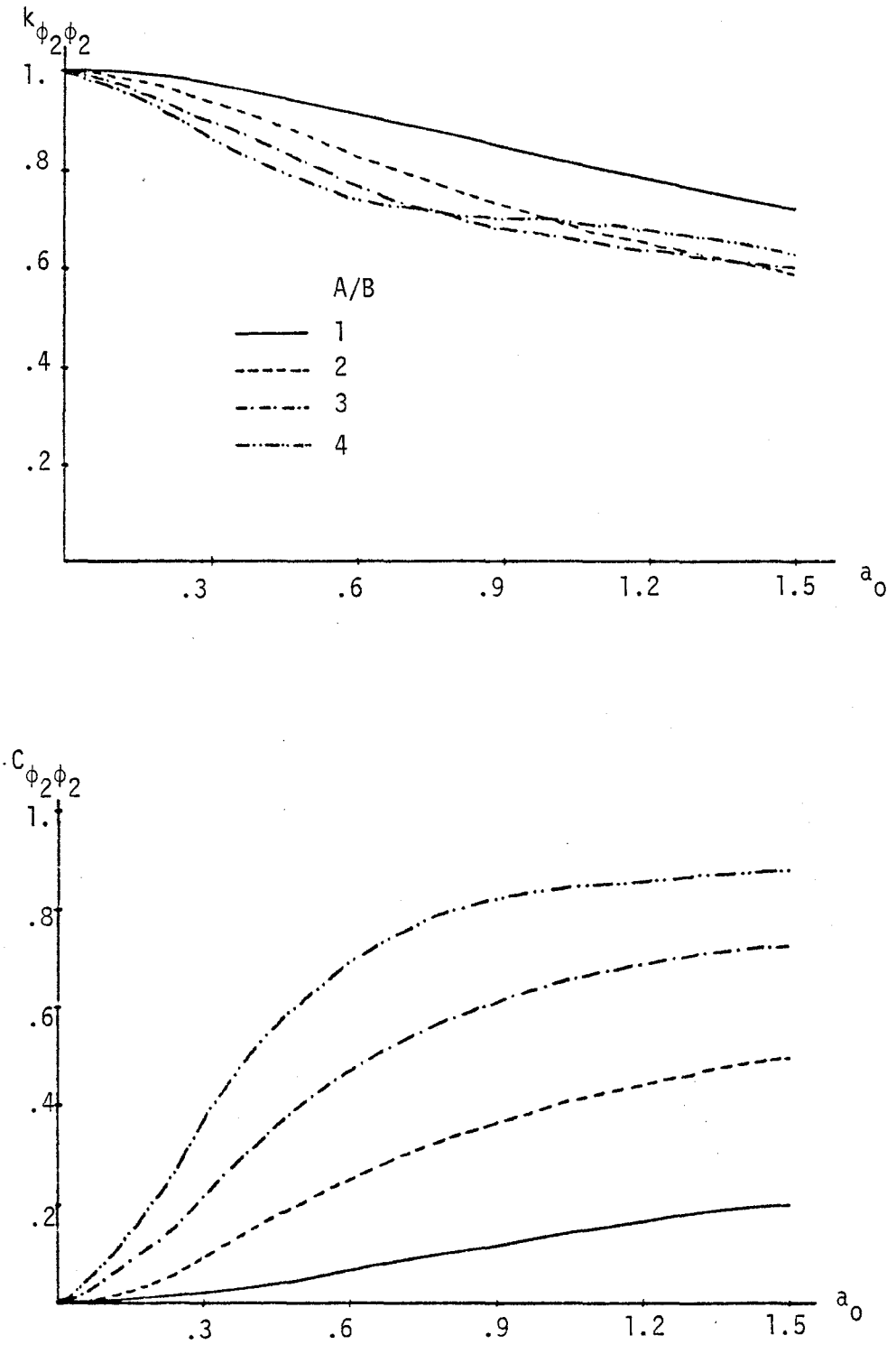

Figure 15 - Rocking Stiffness Coefficients.

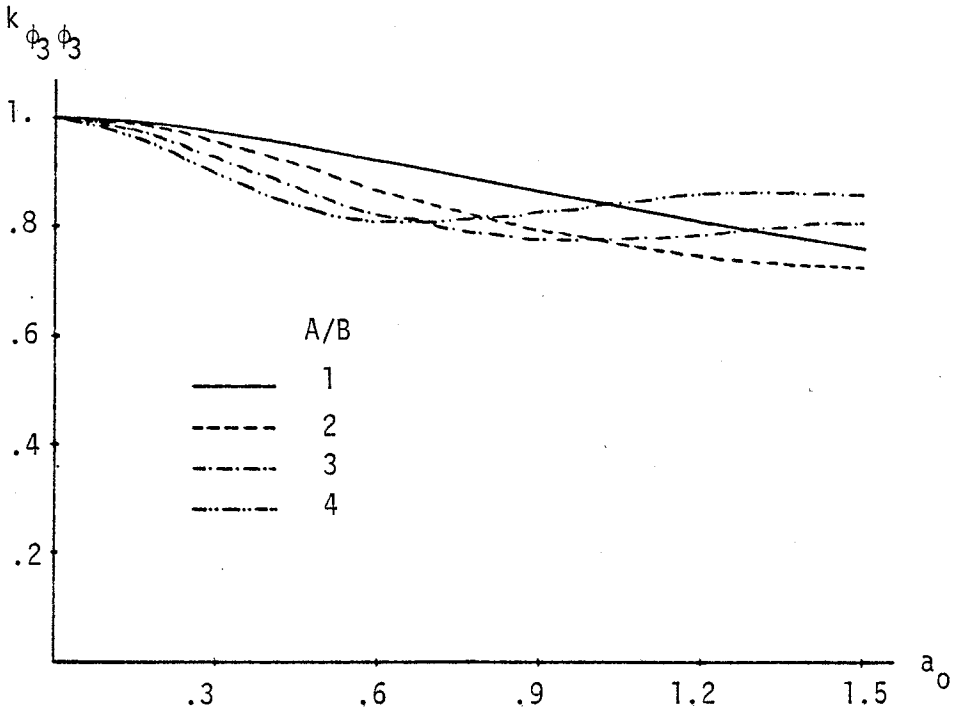

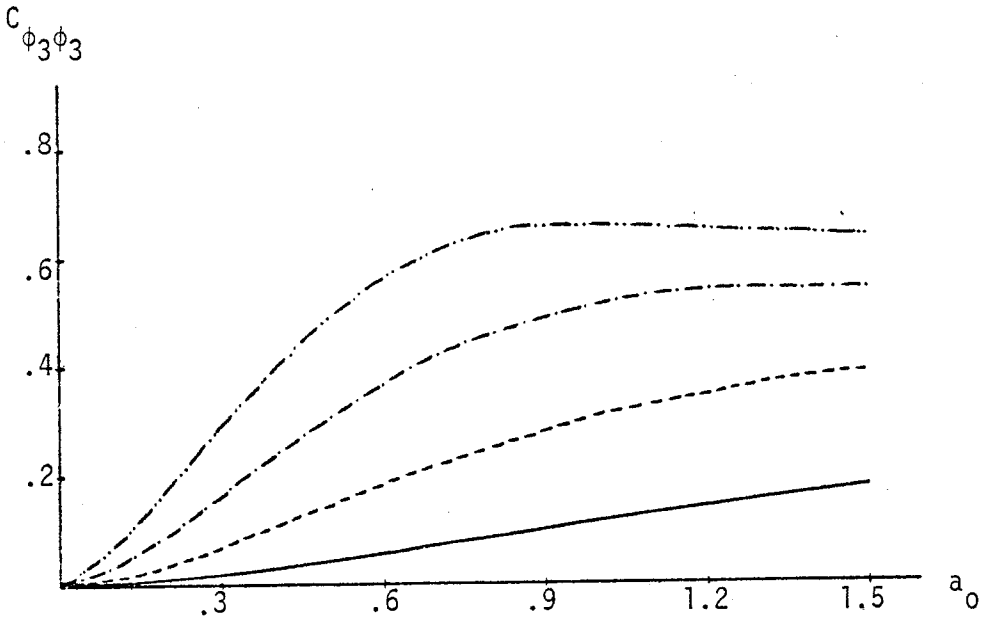

Figure 16 - Torsional Stiffness Coefficients.

Chapter 4

EMBEDDED FOUNDATIONS

Dynamic stiffnesses for embedded square and rectangular foundations were also computed assuming relaxed boundary conditions. The free field was modeled with a band of 16 rectangular elements around the foundation as shown in Figure 17. In order to check the model, some results were obtained with non-relaxed boundary conditions and also considering a bigger zone of the free field. In Table II, results are listed for a square foundation with an embedment ratio E/B = 2/3 being the soil-foundation interface discretized in the same form for all cases, with 3×3 square elements at the bottom and a row of these elements for the side walls. Results are listed for a dimensionless frequency a_o = 0.9, and only 16 free-field elements were considered when using relaxed boundary conditions. When non-relaxed boundary conditions were assumed, the free field was discretized with 16 and 40 rectangular elements, the latter covering a square surface the side of which is seven times the side of the foundation.

TABLE II - EMBEDDED SQUARE FOUNDATION
E/B = 2/3, a_o = 0.9

	Relaxed B.C. 16-free-field elem.	Non-relaxed B.C. 16 free-field elem.	Non-relaxed B.C. 40 free-field elem.
$Re[K_{xx}]/GB$	9.772	9.841	9.627
$Im[K_{xx}]/GB$	8.879	8.922	9.606
$Re[K_{zz}]/GB$	8.650	7.930	8.367
$Im[K_{zz}]/GB$	10.023	9.740	10.573
$Re[K_{\phi_1\phi_1}]/GB^3$	8.987	9.146	9.378
$Im[K_{\phi_1\phi_1}]/GB^3$	2.811	3.105	3.428
$Re[K_{\phi_3\phi_3}]/GB^3$	17.47	17.452	17.289
$Im[K_{\phi_3\phi_3}]/GB^3$	3.895	3.882	4.325

The rocking stiffness for relaxed boundary conditions is always computed by addition of the results for two motions: one that includes the vertical displacements of the bottom and side walls, and the other corresponding to the horizontal motion of the elements on the side walls due to the rotation. The above table shows little variation of results when non-relaxed boundary conditions are considered, and when more elements are added to the free field.

The variation of the static stiffnesses with level of embedment for square foundations, shown in Figure 18, was studied using relaxed boundary conditions, 16 elements on the free field and subdividing the soil-foundation interface into two possible meshes for each level of embedment: one with 3×3 equal square elements on the bottom of the foundation, and the other with 4×4 elements. The side-walls were discretized with one, two or three rows of 12 elements equal to those on the bottom for the first case, and with one, three and four rows of 16 equal rectangular or square elements for the second type of mesh. When the mesh with 4×4 elements on the bottom of the foundation is used for E/B = 2/3 or 4/3, the side-wall elements are not exactly the same as the bottom ones, but for all three levels of embedment considered (E/B = 2/3, 4/3 and 2), the extrapolation law was assumed to be the same as for surface foundation (linear with the size of the bottom elements for the displacement components and quadratic for the rotation and cross-coupling terms).

The comparison of the results in Figure 18 with those for circular foundations is not easy, due to the fact that the equivalent radius of the circular footing is not well defined. A crude comparison shows these results to be close to the ones obtained by Kaldjian [11] for circular embedded foundations.

Figure 19 shows the variation of the horizontal stiffness coefficients with frequency for various values of E/B. The decay with frequency of the term K_{xx} increases with the level of embedment. The term C_{xx} does not change much with frequency for any level of embedment, but it takes higher values as E/B increases. A similar variation with E/B is exhibited by the vertical stiffness coefficients in Figure 20, but the vertical terms have more variation with frequency than the horizontal ones.

Figure 21 presents the variation of the rocking coefficients. It should be noticed that the term $C_{\phi_1\phi_1}$ does not tend to zero in the low range of frequencies when the foundation is embedded. The increase of this term with E/B is similar for the whole range of frequencies represented. The torsional stiffness coefficients shown in Figure 22 have less variation with the level of embedment than the other coefficients, and this variation, as could be expected, is smaller when E/B takes increasing values.

Figure 23 shows the variation of real and imaginary parts of the cross-coupling stiffnesses normalized with respect to the horizontal static stiffness. It can be noticed that the influence of the level of embedment over the real part tends to be smaller as the frequency increases. In Figure 24 the height of the center of stiffness is represented versus frequency and level of embedment. This height has very little variation with both parameters, and for practical purposes it can be assumed to remain constant at h/E = 1/3. The same value was obtained by Kausel [12] for a circular foundation with E/R = 1.

The variation of the real part of the stiffnesses is shown in Figure 25, normalizing all the stiffnesses with respect to the static values for the surface foundation instead of using for each level of embedment its own static value. In this form it can be seen that the influence of the embedment over the real part of the stiffnesses decreases with increasing values of the frequency for the range represented in the figure. This fact was already pointed out for the cross-coupling term.

In order to make this study more general, stiffnesses were also computed for a rectangular embedded foundation with A = 2B and embedment ratios E/B = 2/3 and 4/3. Relaxed boundary conditions were assumed, and the free field was modeled again with a band of rectangular elements (this time 22) around the foundation.

The variation of the static stiffnesses with embedment ratio was studied again using two meshes to discretize the soil-foundation interface, one with 3×6 elements at the bottom, and the other 4×8. The side-walls were modeled with one or two rows of 18 square elements around the bottom for

the first kind of mesh, and one or two bands of 24 equal rectangular elements with an aspect ratio of 4/3 for the second type of mesh. The extrapolation laws were the same as for the square foundation. Figure 26 shows the variation of the static stiffnesses with level of embedment, and it can be noticed that this variation is of the same shape as for the square foundation. The increase with E/B is, however, smaller, as could be expected, due to the fact that the level of embedment is measured versus the small side B.

Figures 27 to 32 show the variation of stiffness coefficients with the dimensionless frequency a_o for the two levels of embedment considered, and for the surface foundation. The variation of those coefficeents with embedment is in general of the same shape as for the square foundation. Both rocking damping coefficients $C_{\phi_1\phi_1}$ and $C_{\phi_2\phi_2}$ have again non-zero values for the embedded foundations when ω tends to zero, but the term $C_{\phi_2\phi_2}$ has a smaller increase with E/B than $C_{\phi_1\phi_1}$, and a larger variation with frequency for all values of E/B.

The cross-coupling terms are presented in Figures 33 and 34. Both have essentially the same behavior. Figure 35 shows the height of the center of stiffness in both directions. The values are almost the same and remain approximately h/E = 1/3.

Figure 36 shows the real part of the dynamic stiffnesses normalized with respect to the static value for the surface foundation and as in the square case it can be noticed that the influence of the level of embedment on the real part of the stiffnesses becomes smaller as a_o increases in the range represented.

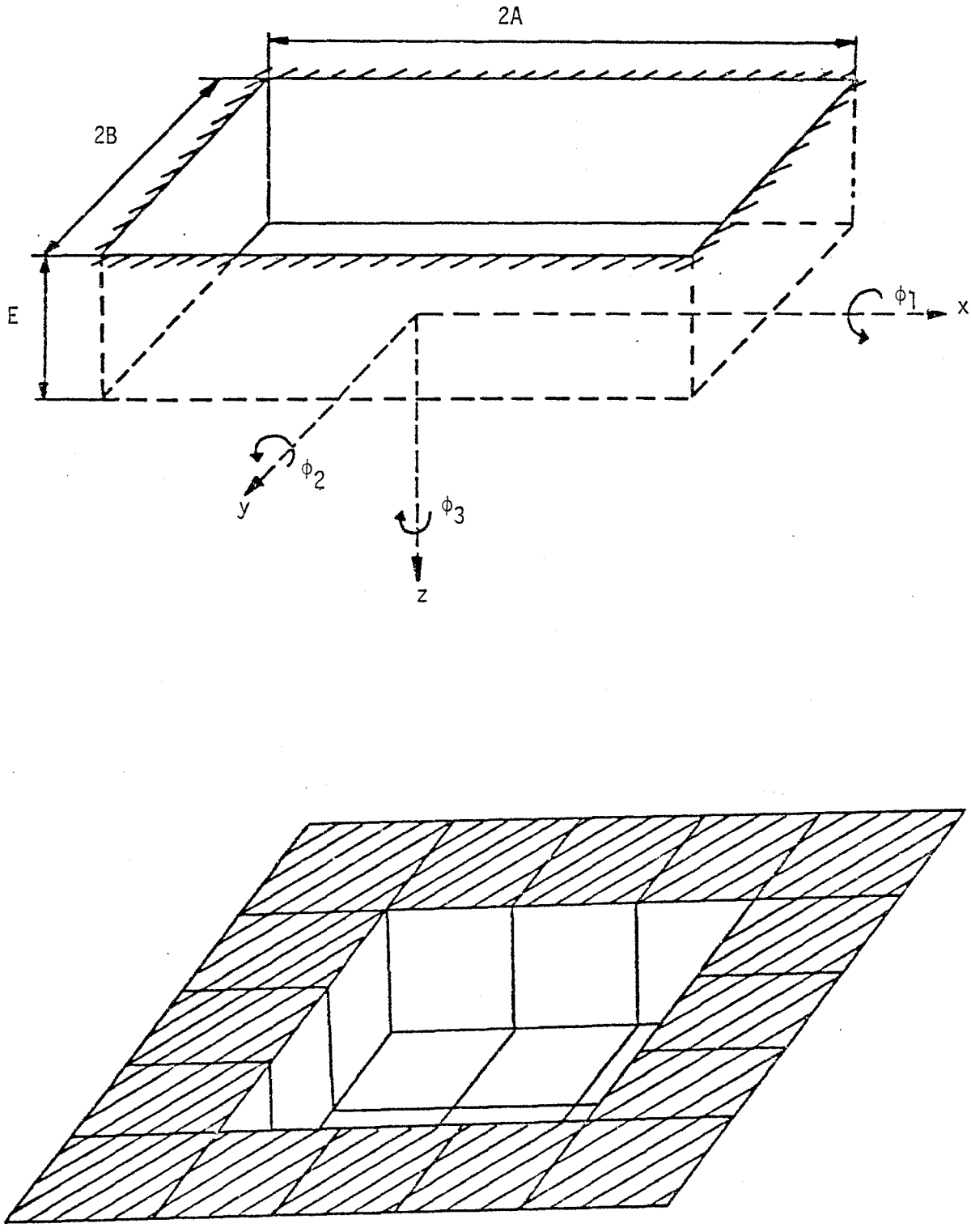

Figure 17 - Type of Model and System of Coordinates for Embedded Rectangular Foundations.

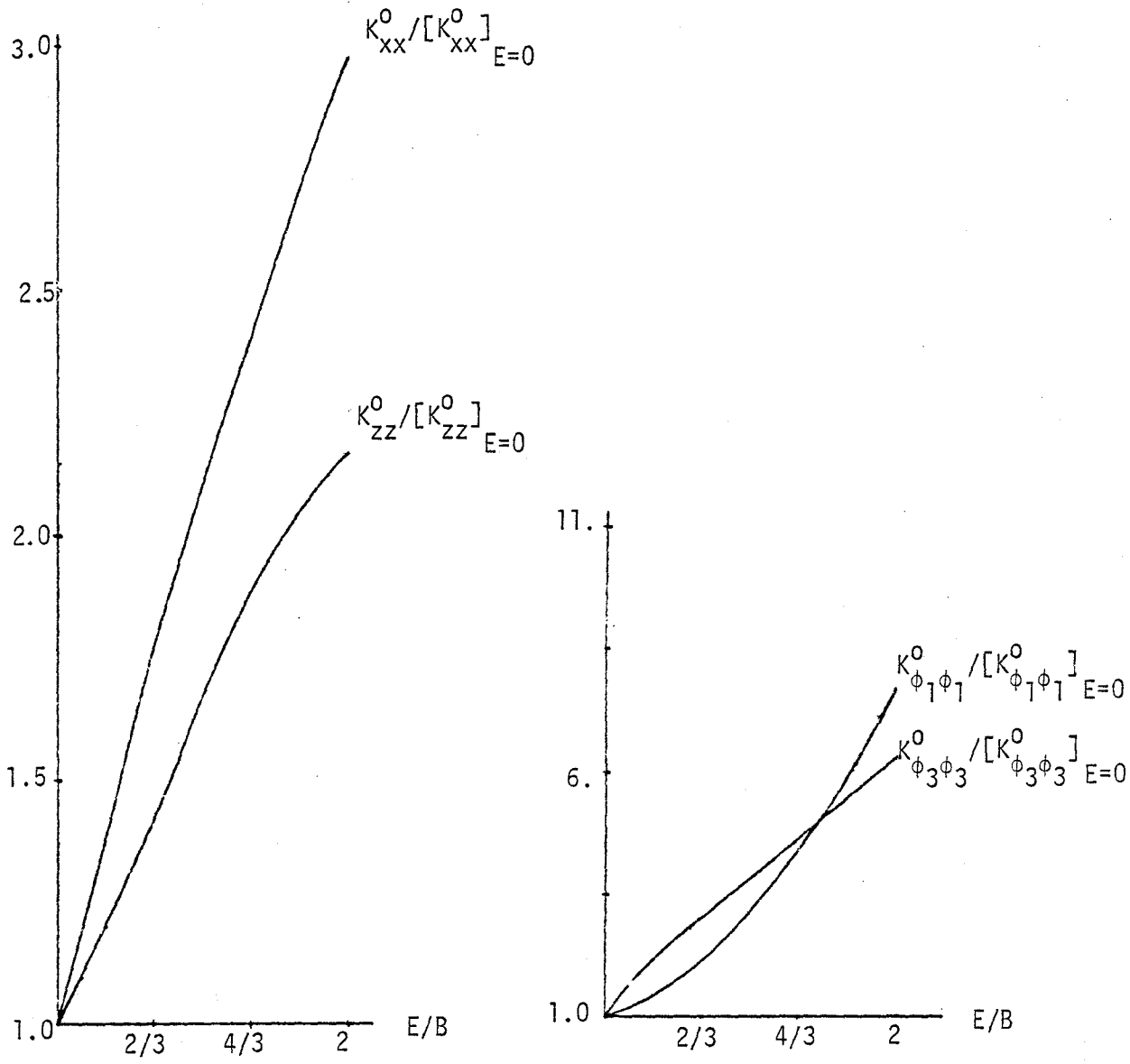

Figure 18 - Static Stiffness for Embedded Square Foundations

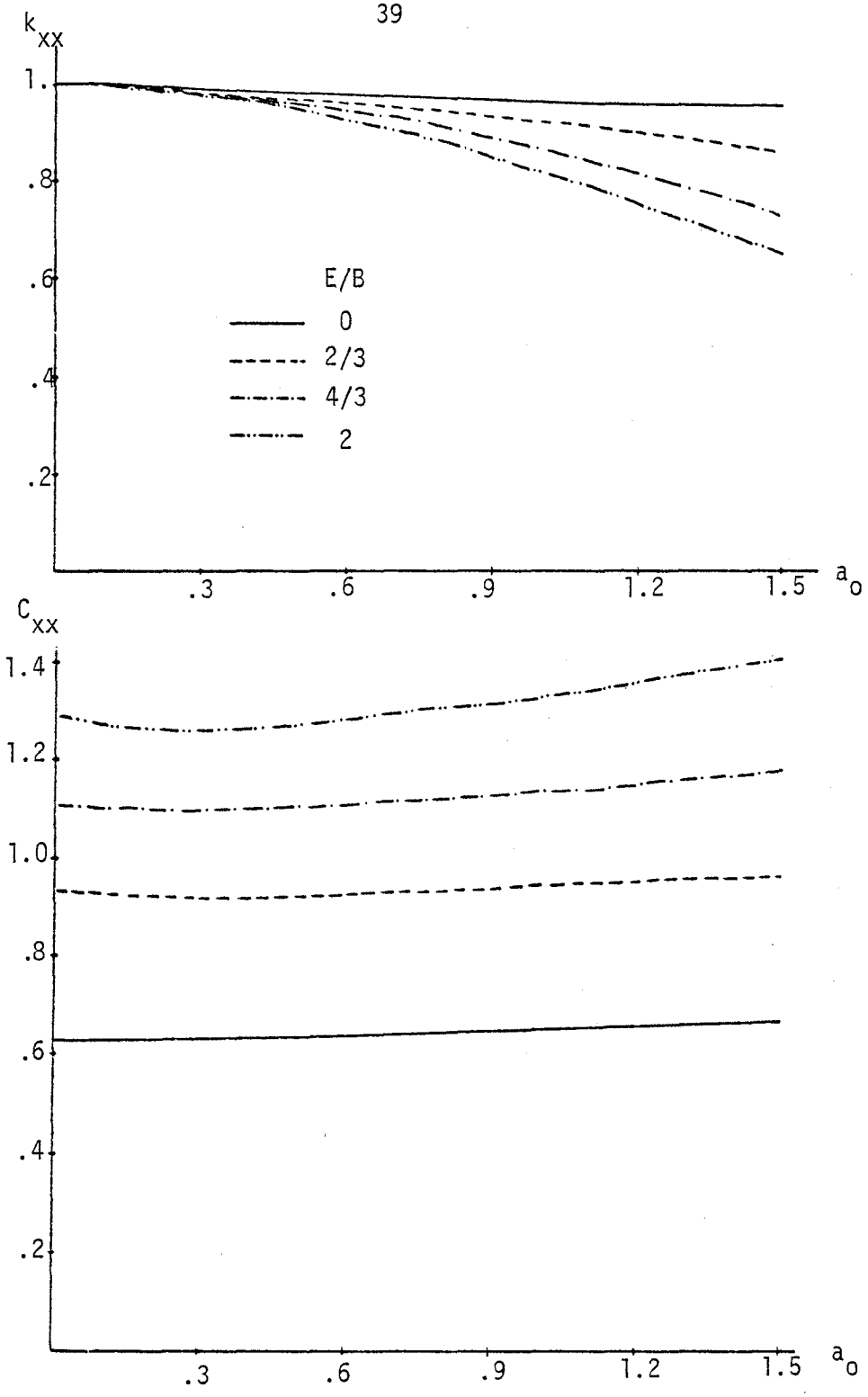

Figure 19 - Horizontal Stiffness Coefficients. Square Embedded Foundation.

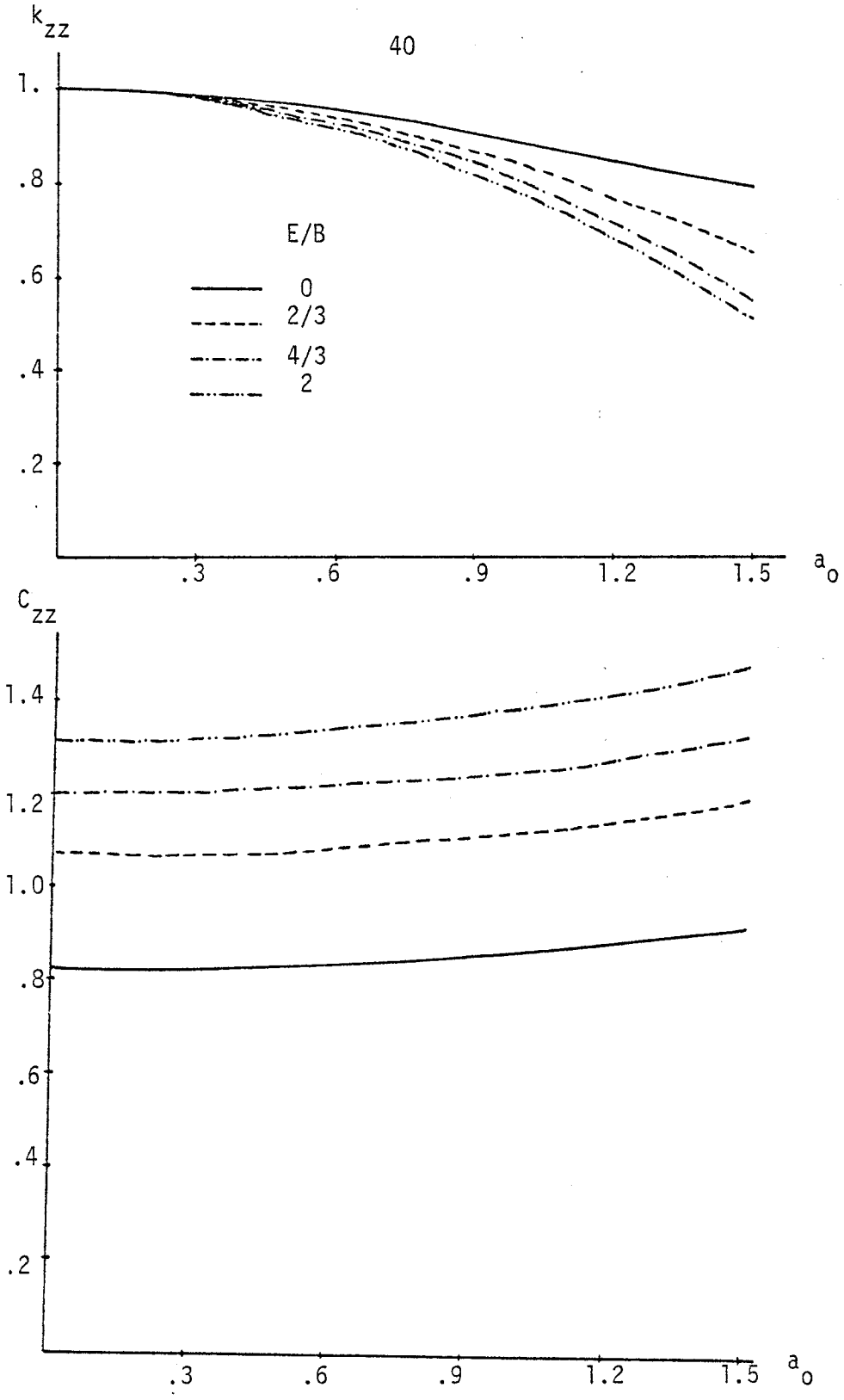

Figure 20 - Vertical Stiffness Coefficients. Square Embedded Foundation.

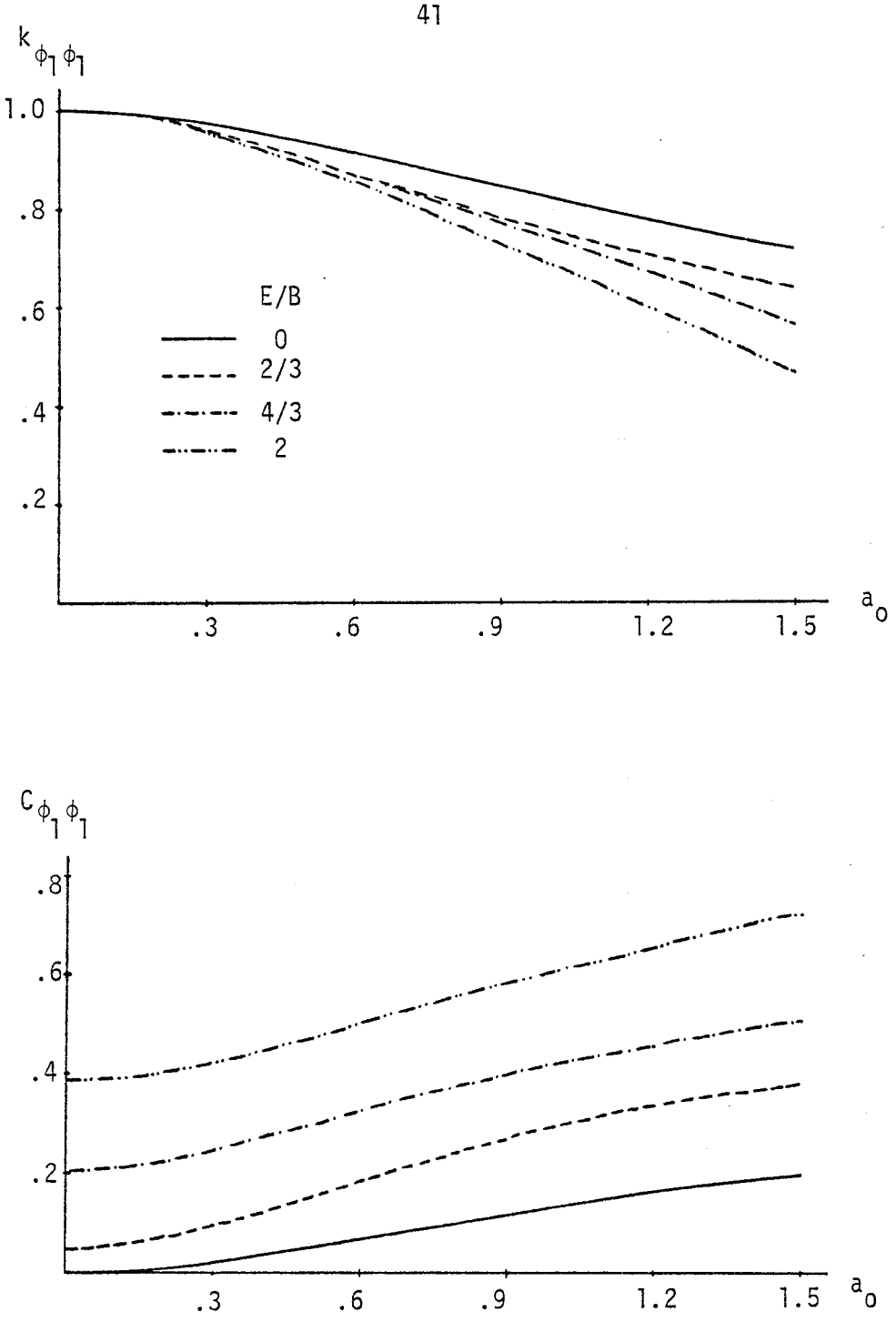

Figure 21 - Rocking Stiffness Coefficients. Square Embedded Foundation.

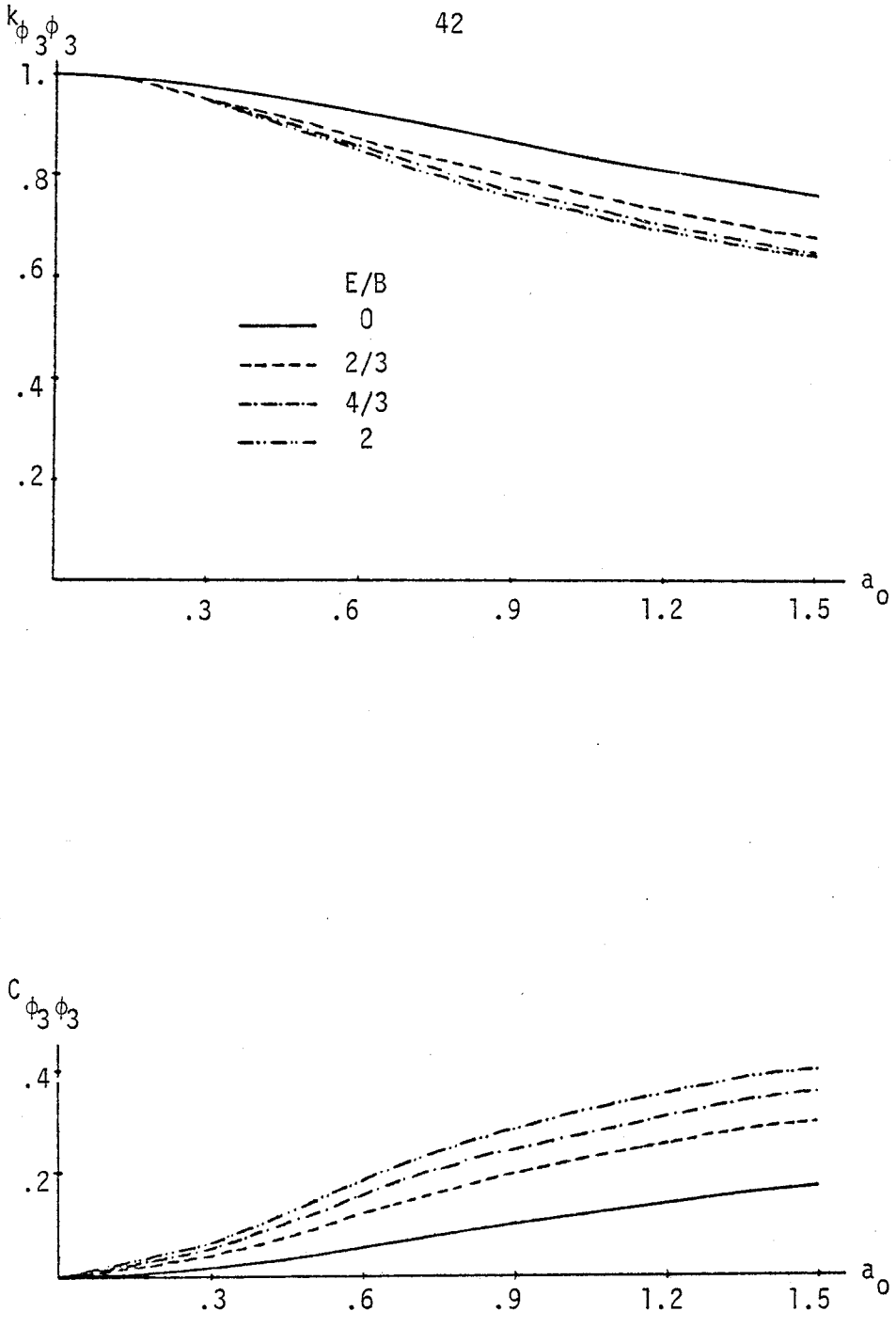

Figure 22 - Torsional Stiffness Coefficients. Square Embedded Foundation.

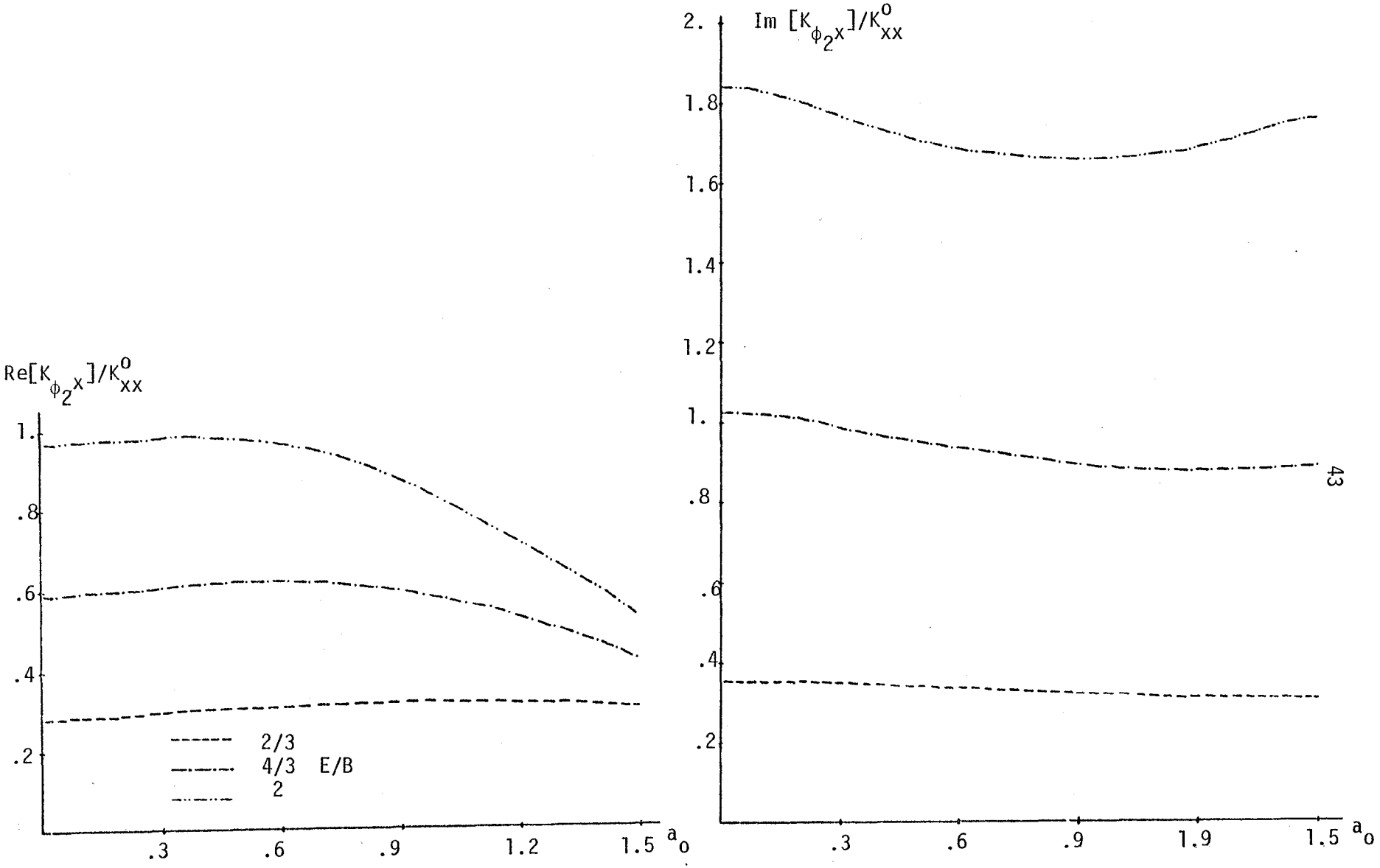

Figure 23 - Cross Coupling Stiffness. Square Embedded Foundation.

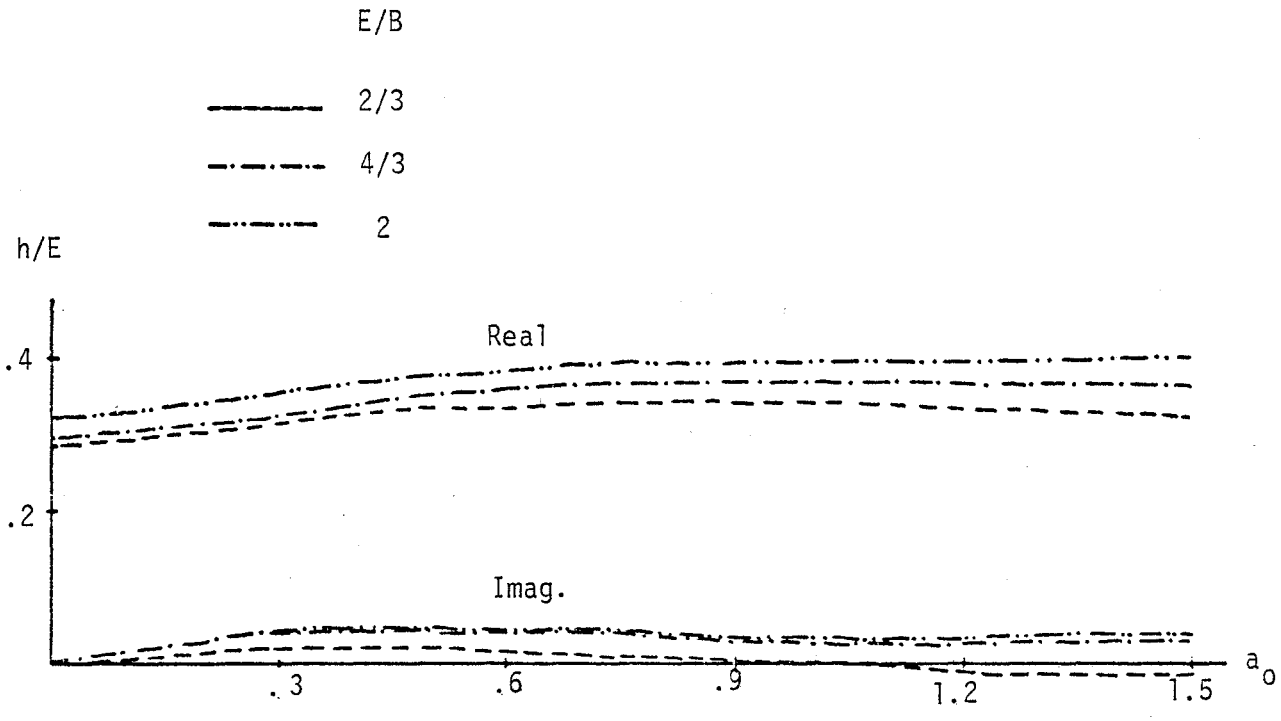

Figure 24 - Height of the Center of Stiffness for Square Embedded Foundation.

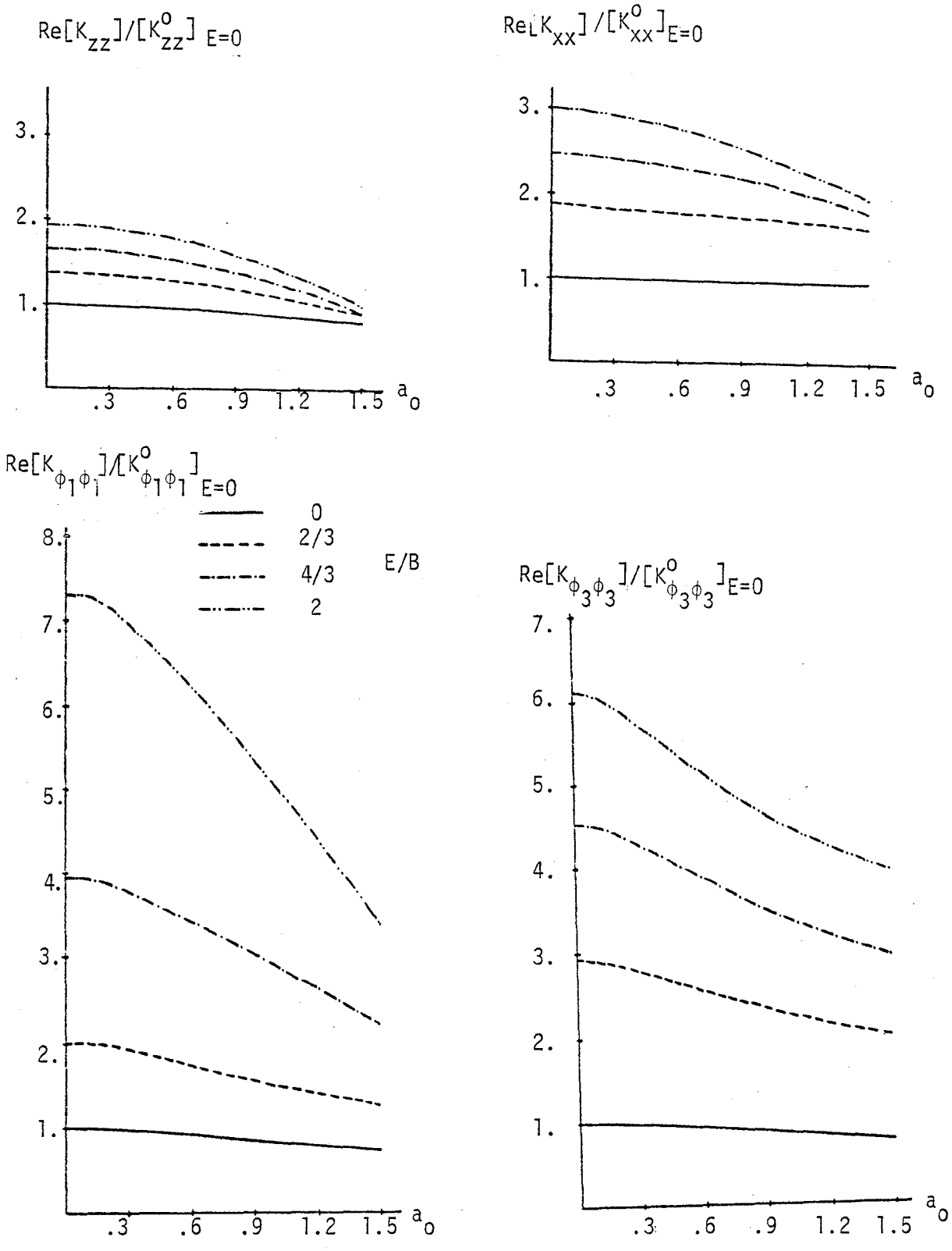

Figure 25 - Real Component of the Stiffness for Square Embedded Foundation.

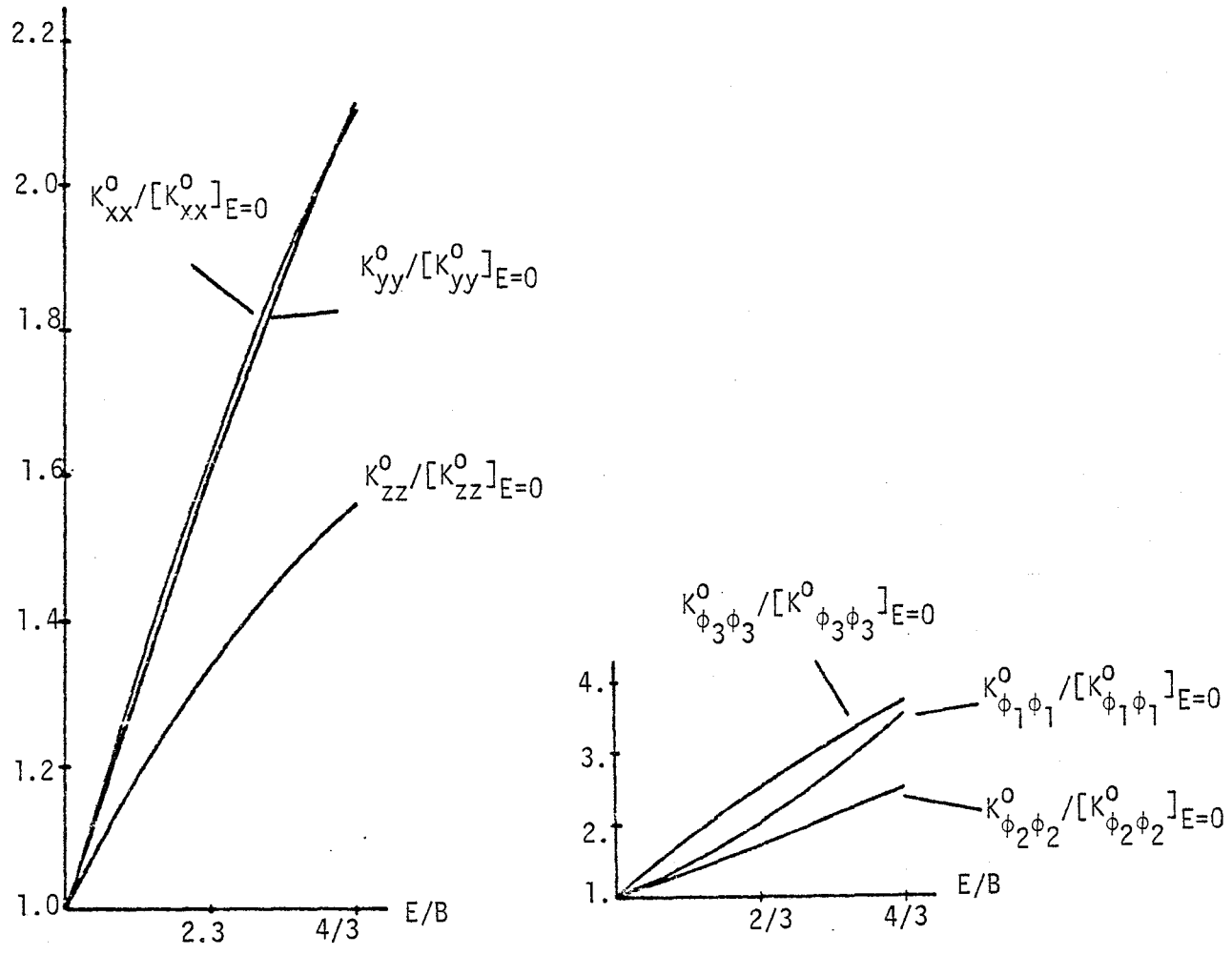

Figure 26 - Static Stiffness for Embedded Rectangular Foundation. A = 2B.

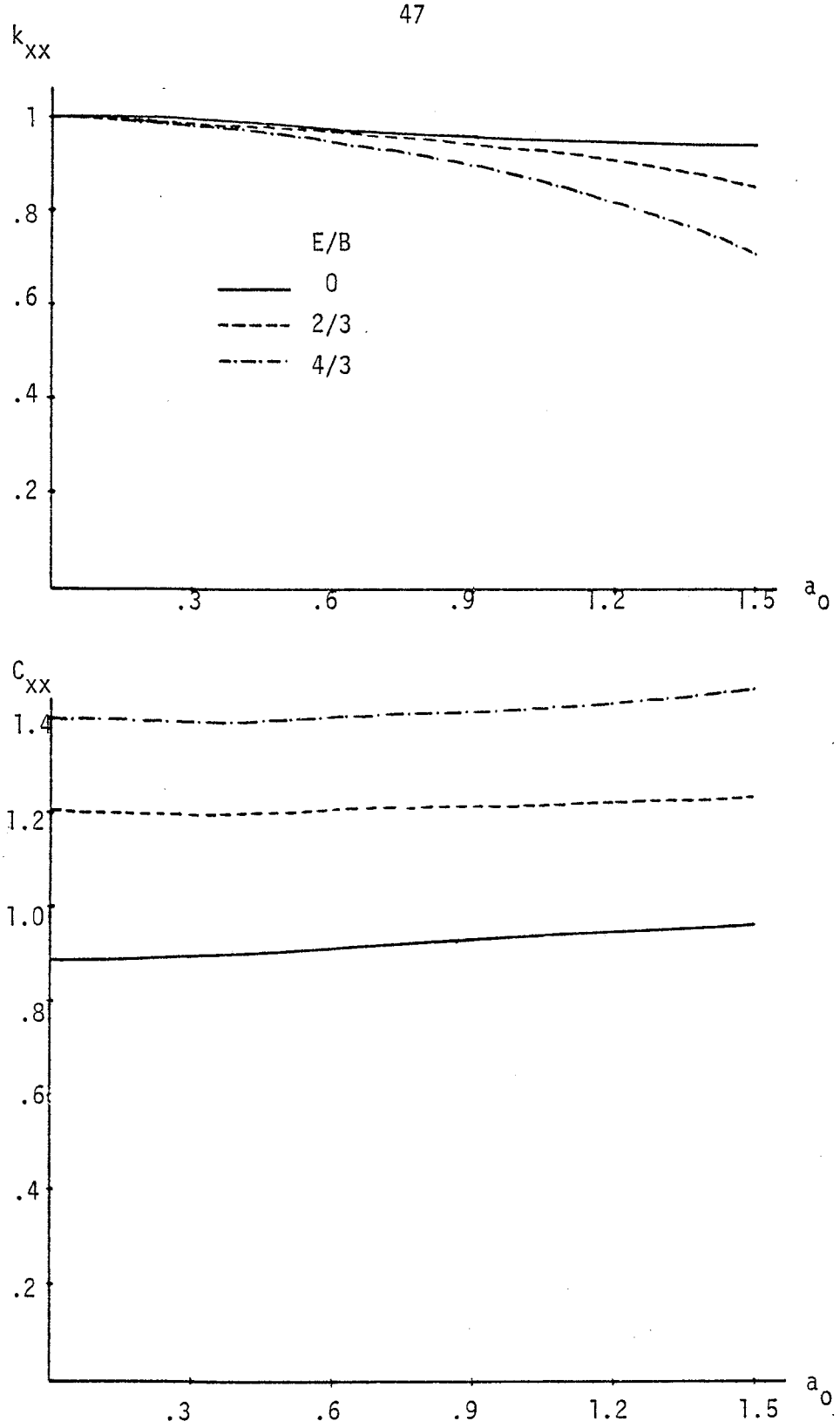

Figure 27 - Horizontal Stiffness Coefficients. Rectangular Foundation. A = 2B

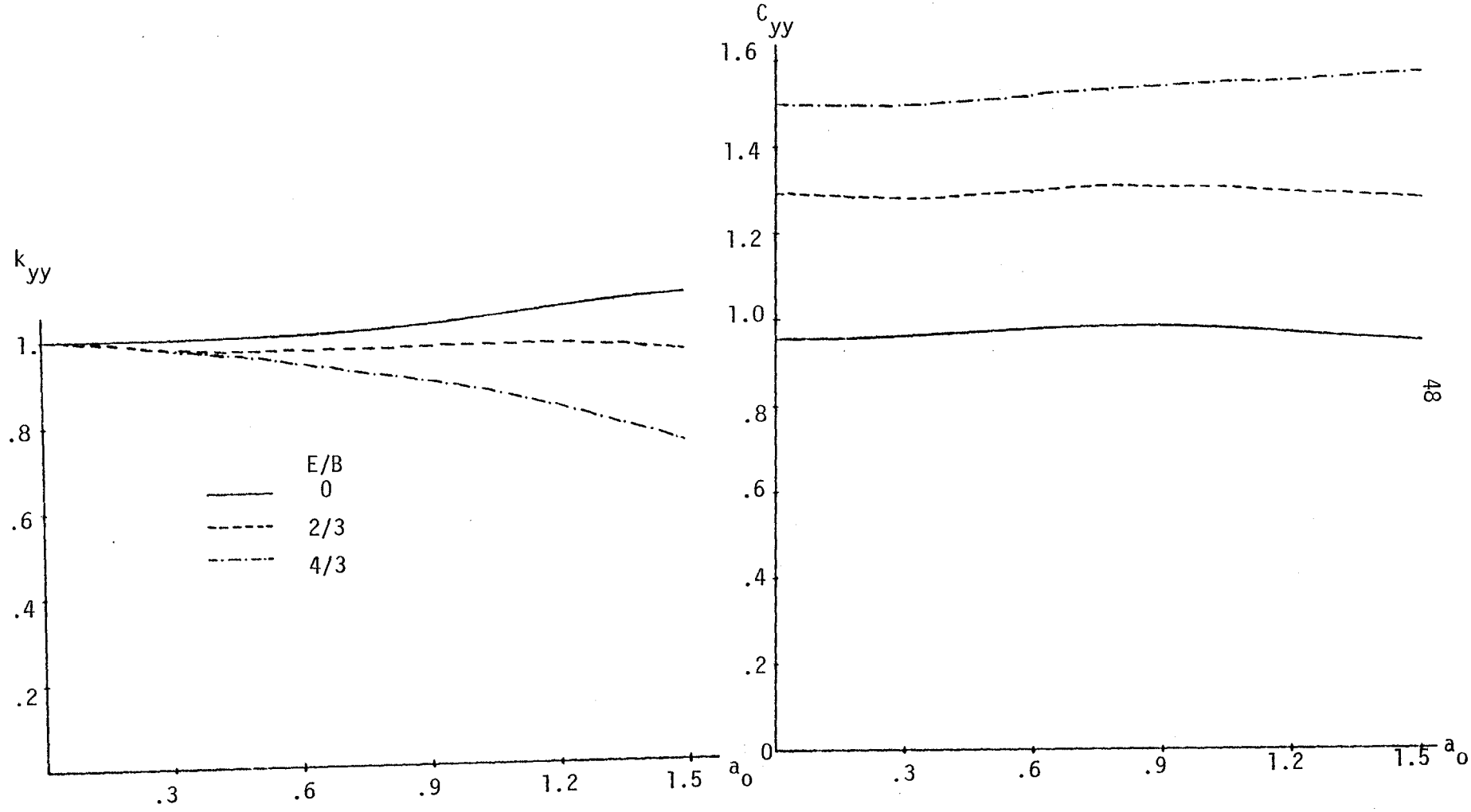

Figure 28 - Horizontal Stiffness Coefficients. Rectangular Foundations. A = 2B.

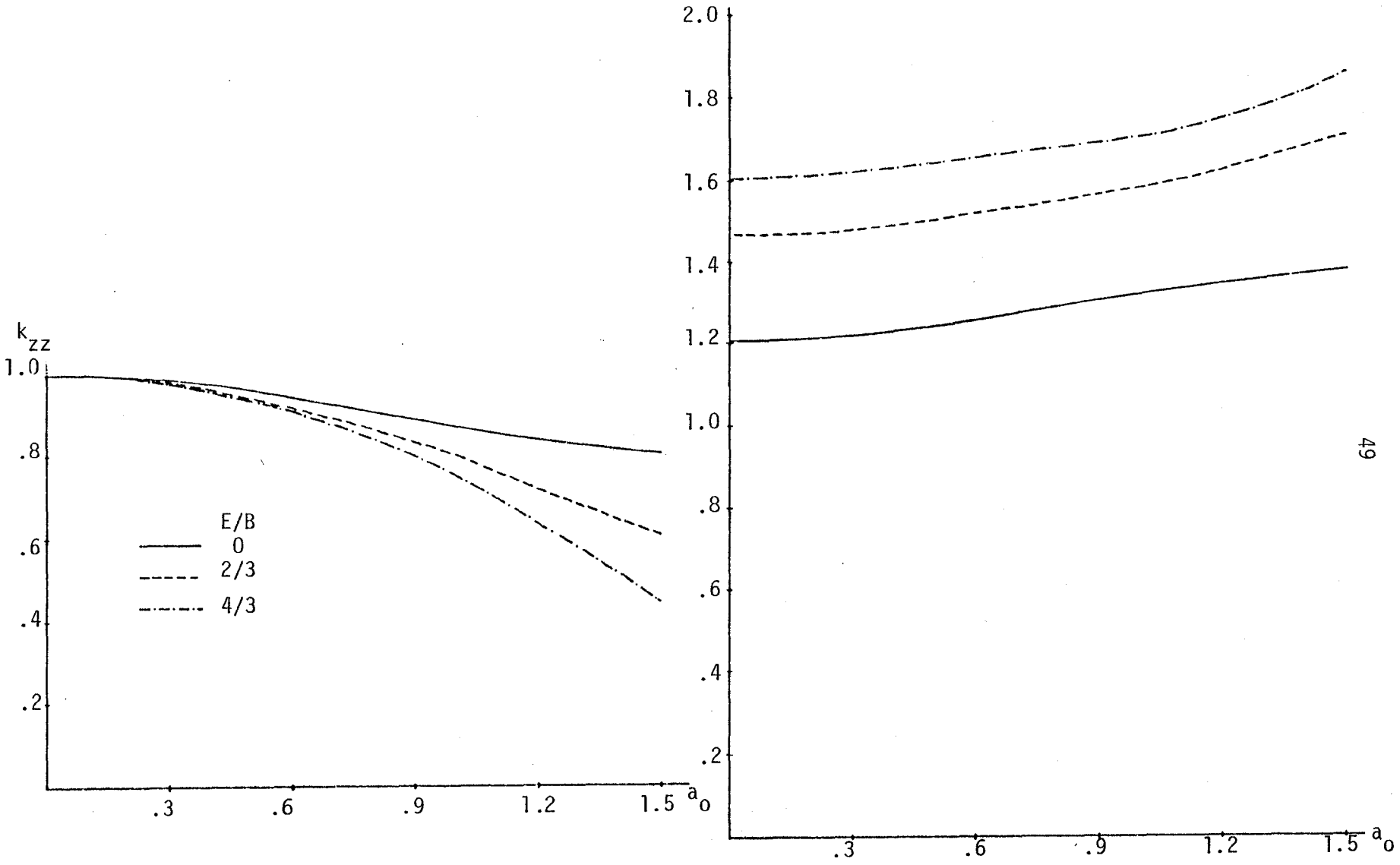

Figure 29 - Vertical Stiffness Coefficients . Rectangular Foundations. A = 2B.

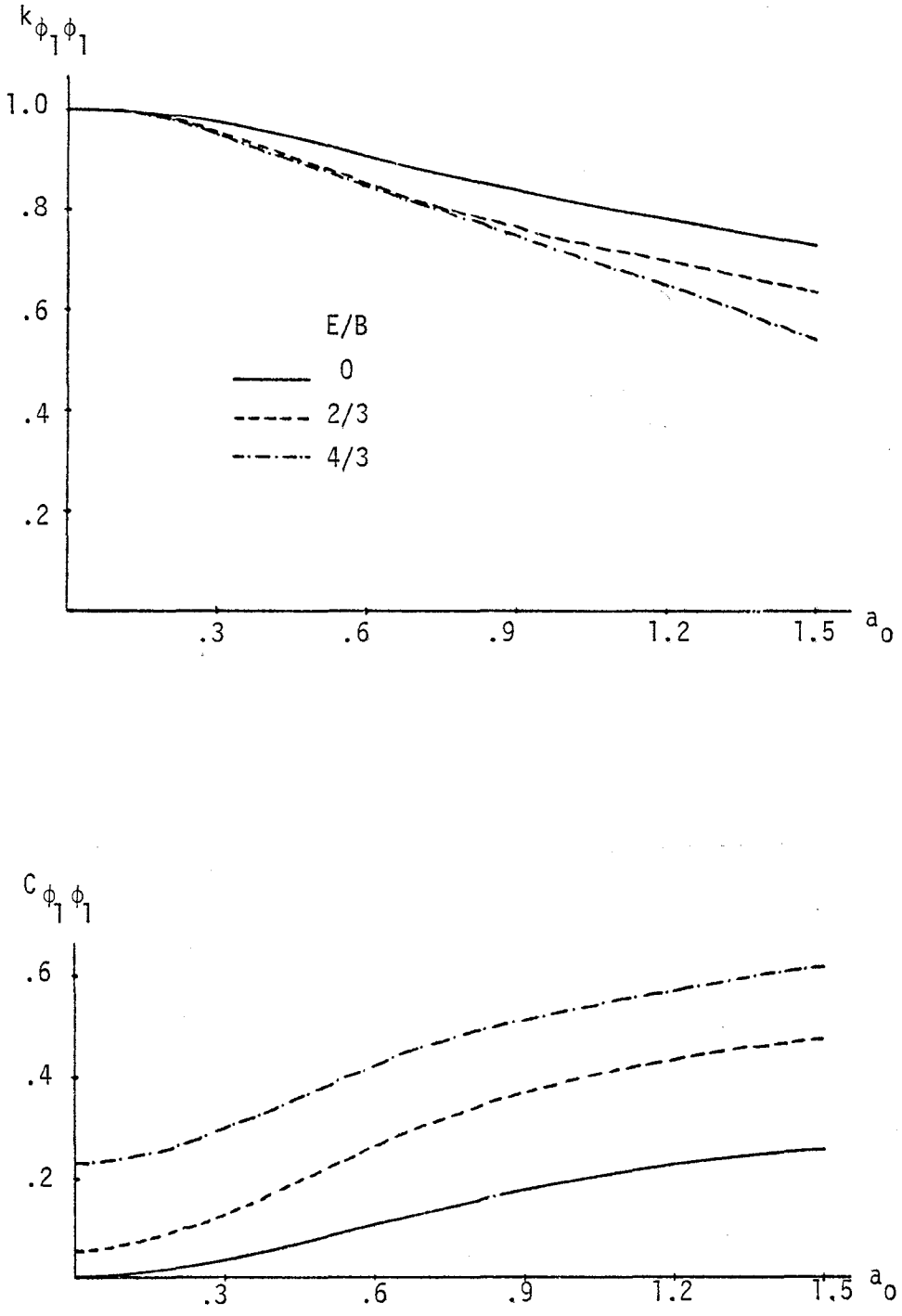

Figure 30 - Rocking Stiffness Coefficients. Rectangular Foundations. A = 2B.

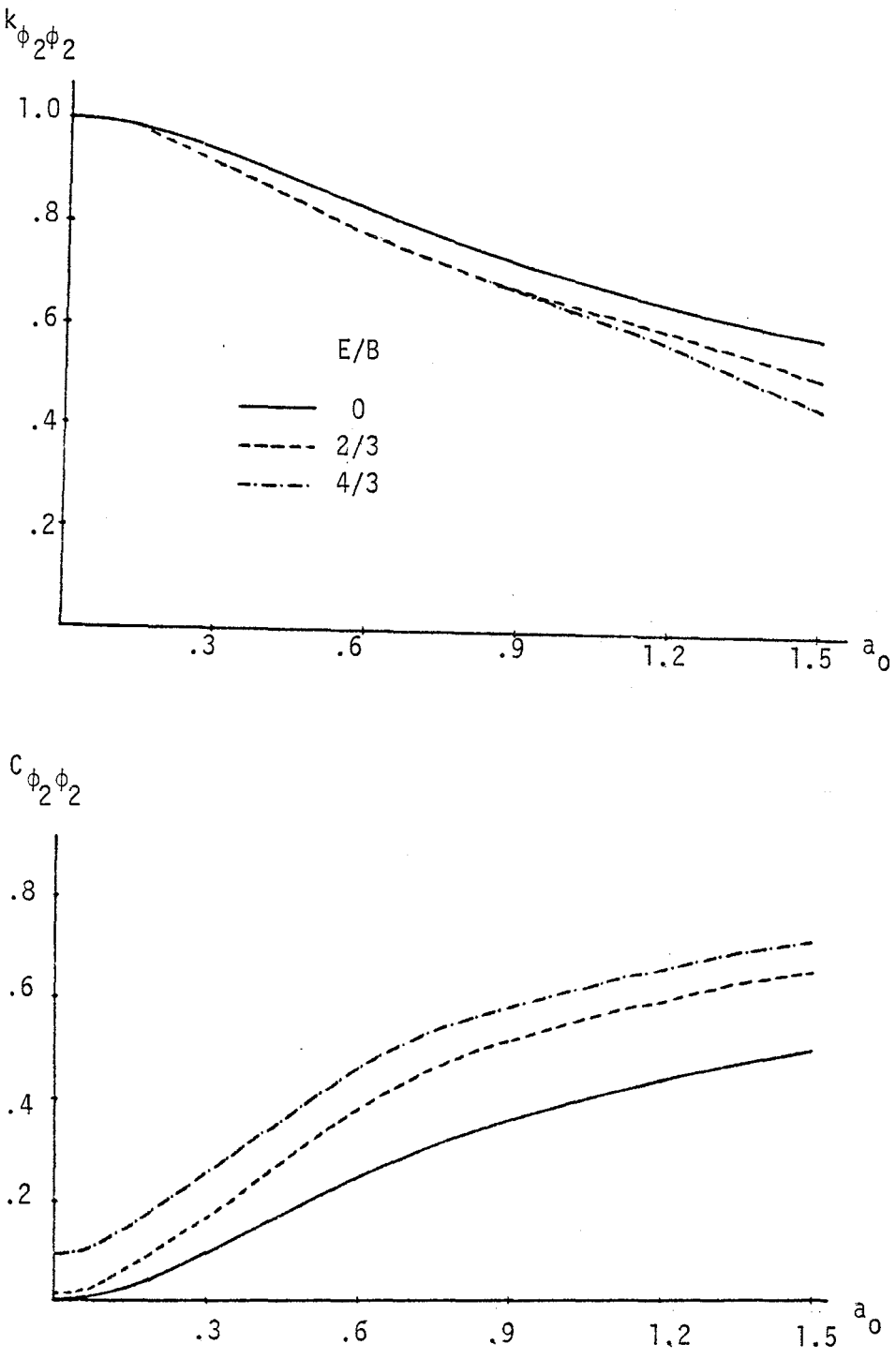

Figure 31 - Rocking Stiffness Coefficients.
Rectangular Foundations. A=2B.

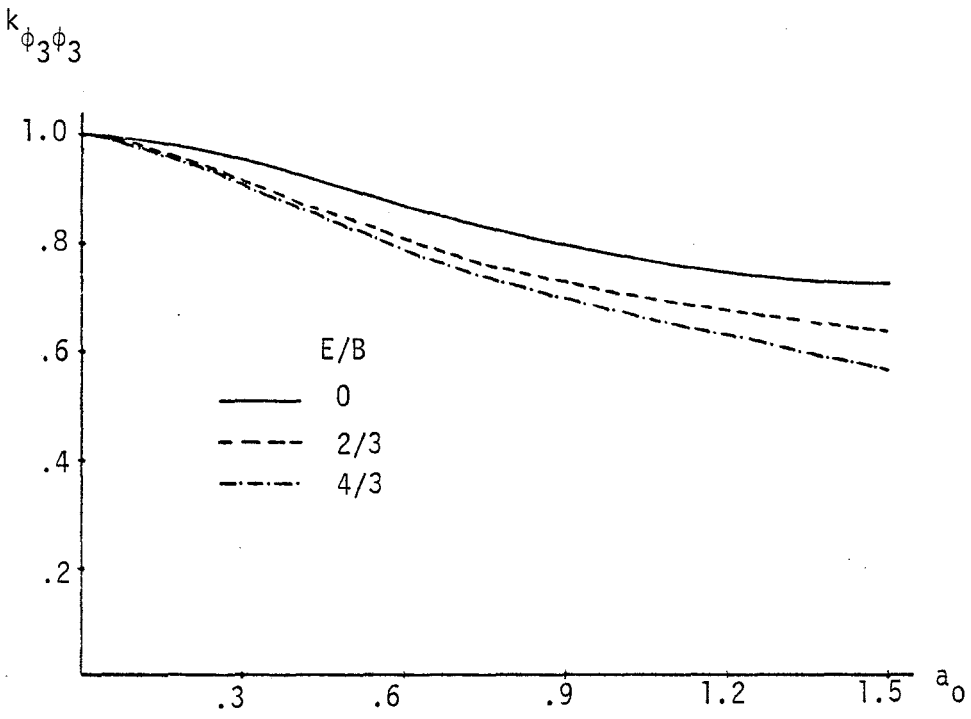

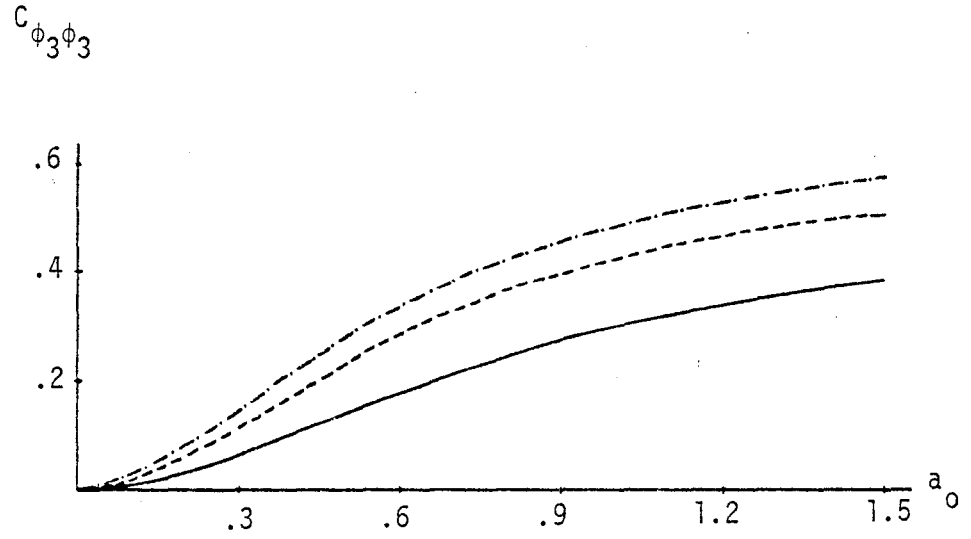

Figure 32 - Torsional Stiffness Coefficients.
Rectangular Foundations. A = 2B.

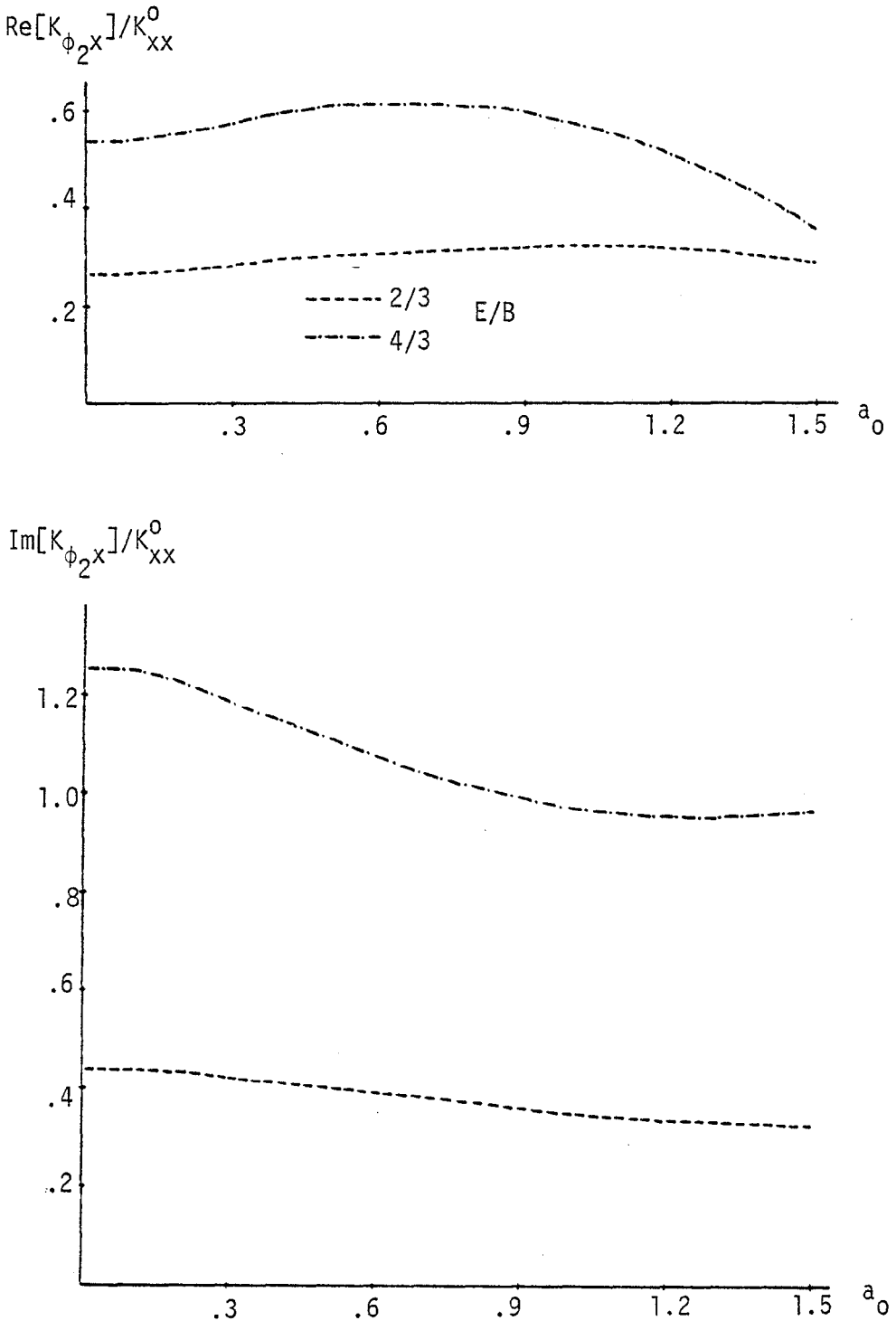

Figure 33 - Cross Coupling Stiffness. Rectangular Foundation. A = 2B.

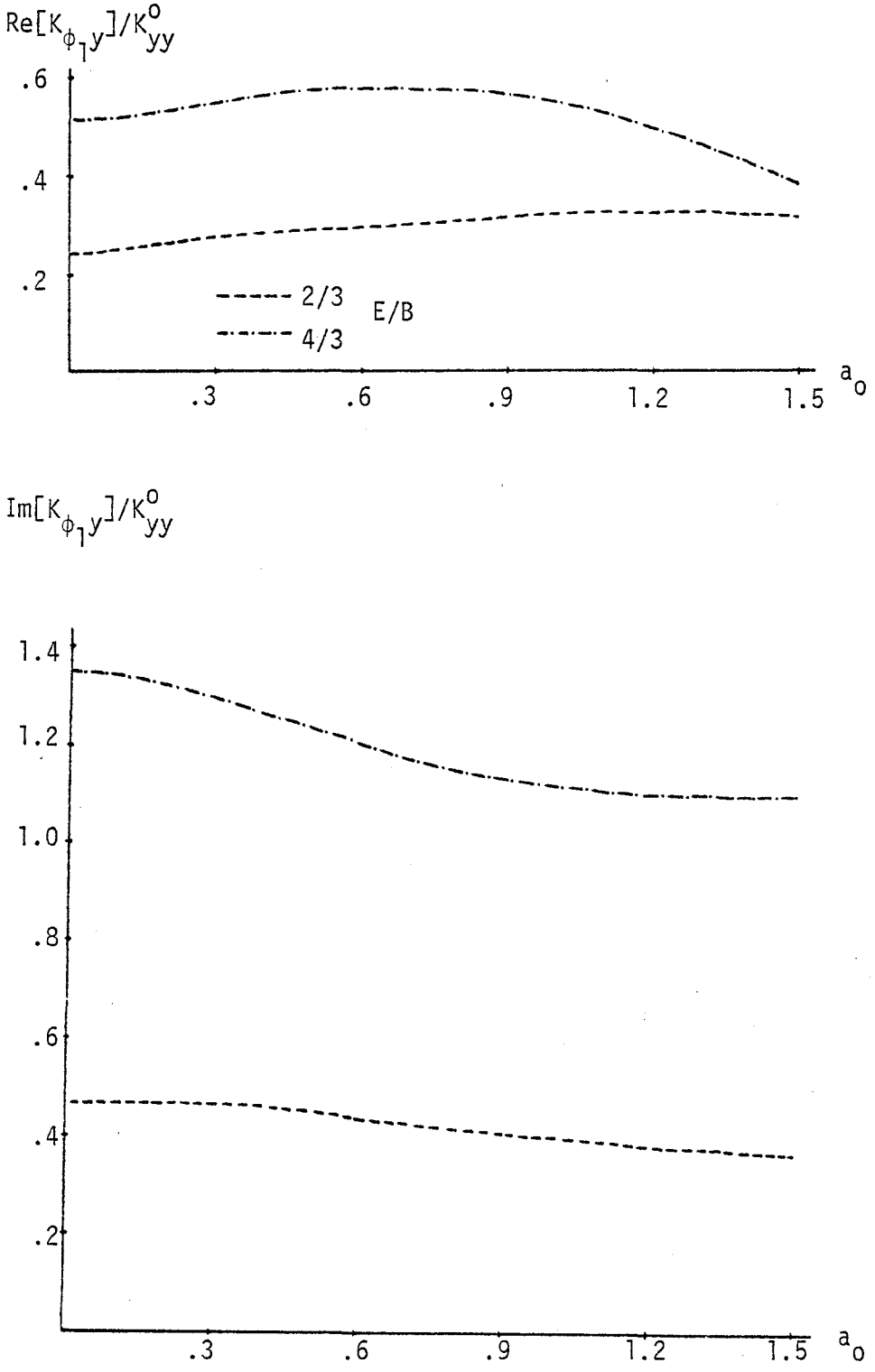

Figure 34 - Cross Coupling Stiffness. Rectangular Foundations. A = 2B.

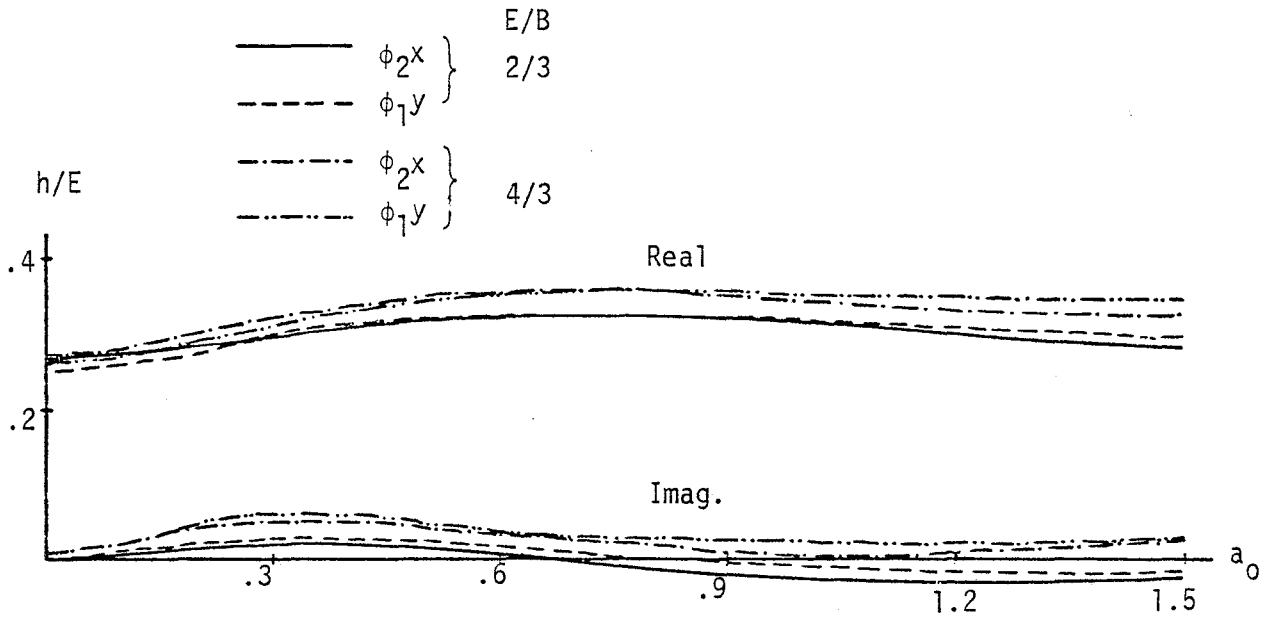

Figure 35 - Height of the Center of Stiffness.
Rectangular Foundation. A = 2B.

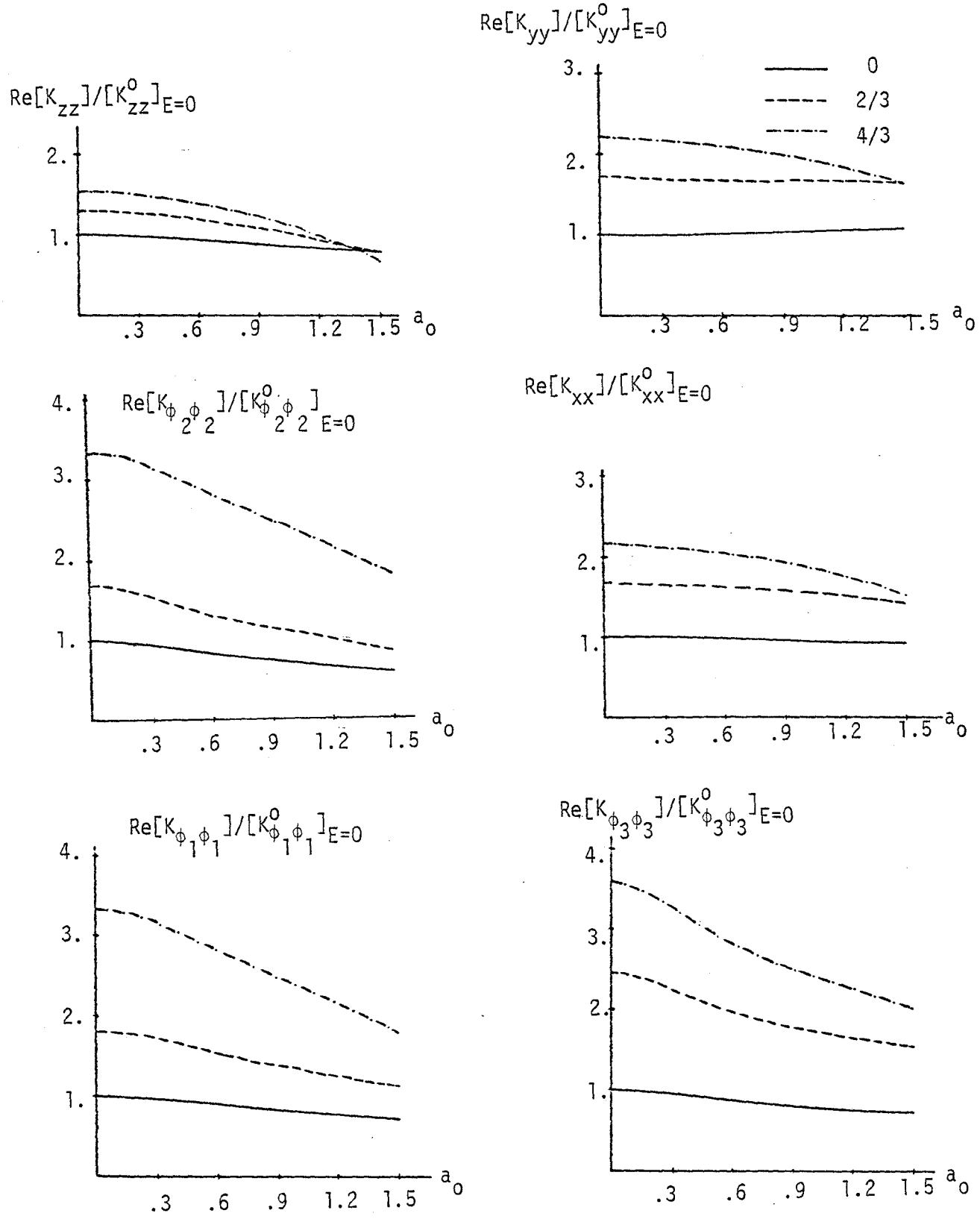

Figure 36 - Real Component of the Stiffness. Rectangular Foundation. A = 2B.

Chapter 5

CONCLUSIONS AND RECOMMENDATIONS

One of the purposes of this work was to explore the applicability of the Boundary Element method to the solution of problems in the area of Soil Dynamics. Because only the boundary of the region of interest has to be discretized instead of the whole domain, the method reduces the dimensions of the problem by one over classical finite element solutions. On the other hand the resulting boundary matrices are full instead of exhibiting a band. The method is as a result particularly attractive when dealing with a three-dimensional situation, an elastic or viscoelastic halfspace and embedded foundations of arbitrary shape.

A second problem encountered is that there is no closed form analytical solution for the displacements and stresses due to a concentrated load inside a halfspace. It was found, however, that by using the expressions corresponding to the full space, accurate and economical solutions could still be obtained. For surface foundations with relaxed boundary conditions (smooth footing), it is only necessary to consider the boundary under the foundation. For all other cases one must include part of the soil surface outside of the foundation, but only a small number of elements in this region are needed to obtain satisfactory results.

For surface foundations the results obtained were compared to those published by other researchers. The agreement with the solutions of Wong and Luco was very good at approximately one third of the computation cost reported by Wong. Agreement with the results for stiffnesses of rectangular foundations obtained by Vardanega using a finite element type formulation was within 5 to 10%. No attempt was made at this stage to derive approximate formulae for the static stiffnesses or the dynamic coefficients as a function of the aspect ratio, but it appears that for the range considered (ratios A/B from 1 to 4) relatively simple expressions could be fitted to the results. The translational and torsional static stiffnesses vary in this range almost linearly with aspect ratio, while the variation of the rocking stiffnesses is parabolic.

The results for embedded foundations confirm in general terms those reported by Elsabee for circular foundations embedded in a finite soil stratum. Embedment increases the real and imaginary parts of the stiffnesses. The increase of the real part tends to disappear, however, as the frequency increases. For the static case and embedment ratios E/B (E embedment depth, B half of the smaller foundation size) in the order of 1 or less, a linear variation of the stiffnesses (as suggested by Elsabee) would provide a reasonable approximation. The fact that the rocking stiffnesses have a nonzero imaginary part, indicating the existence of radiation damping, even for the static case is a result of particular significance which seems physically correct. This effect could not be detected in Elsabee's work because of the existence of a finite soil stratum on rigid rock (no radiation will take place in this case below the fundamental frequency of the stratum).

The curves included in the report can be used directly or with the help of interpolation to estimate in practice the dynamic stiffnesses of rectangular foundations. It should be noticed, however, that the effect of embedment is actually dependent on the conditions of the backfill. In reality, the assumption of a foundation welded to the surrounding soil may only be valid for small levels of vibrations. When separation occurs the true stiffnesses should be somewhere between those of a surface and an embedded foundation.

References

1. Brebbia, C.A. and Dominguez, J., "Boundary Element Methods for Potential Problems," Applied Mathematical Modelling Journal, December 1977.

2. Cruse, T.A. and Rizzo, F.J., "A Direct Formulation and Numerical Solution of the General Transient Elastodynamic Problem. I", Journal of Mathematical Analysis and Applications, 22, 1968.

3. Cruse, T.A. and Rizzo, F.J., "A Direct Formulation and Numerical Solution of the General Transient Elastodynamic Problem. II", Journal of Mathematical Analysis and Applications, 22, 1968.

4. Doyle, J.M., "Integration of the Laplace Transformed Equations of Classical Elastokinetics," Journal of Mathematical Analysis and Applications, 13, 1966.

5. Elorduy, J., Nieto, J.A. and Szekely, E.M., "Dynamic Response of Bases of Arbitrary Shape Subjected to Periodic Vertical Loading," Proceedings International Symposium on Wave Propagation and Dynamic Properties of Earth Materials, 1967.

6. Gazetas, G. and Roesset, J.M., "Forced Vibrations of Strip Footing and Layered Soils," Proceedings of the National Structural Engineering Conference, ASCE, Vol. 1, 1976.

7. Gonzalez, J.J., "Dynamic Interaction between Adjacent Structures," Research Report R77-30, Dept. of Civil Enginering, M.I.T., September, 1977.

8. Harkreider,D.,"Surface Waves in Multi-Layer Elastic Media. Raleigh and Love Waves from a Body Force," Bulletin of the Seismological Society of America, 54, 1964.

9. Jaswon, M.A. and Ponter, R., "An Integral Equation Solution of the Torsion Problem,"Proceedings of the Royal Society, Series A, p. 273, 1963.

10. Kaldjian, M.J., "Torsional Stiffness of Embedded Footings," Journal of the Soil Mechanics and Foundations Division, ASCE, 97, July 1971.

11. Kaldjian, M.J., discussion of "Design Procedures for Dynamically Loaded Foundations," by Whitman, R.V. and Richard, F.E., Journal of Soil Mechanics and Foundations Division, ASCE, 95, 1969.

12. Kausel, E., "Forced Vibrations of Circular Foundations on Layered Media," Research Report R74-11, Dept. of Civil Engineering, M.I.T., January 1974.

13. Kitamura, Y. and Sakurai, S., "Dynamic Stiffness for Rectangular Rigid Foundations on a Semi-infinite Elastic Medium," International Journal of Numerical and Analytical Methods in Geomechanics, 1978.

14. Lamb, H., "On the Propagation of Tremors over the Surface of an Elastic Solid," Philosophical Trans. Royal Society of London, Series A, 203, 1904.

15. Mindlin, R.D., "Force Point in the Interior of a Semi-Infinite Solid," Physics, 7, May 1936.

16. Rizzo, F.J., "An Integral Equation Approach to Boundary Value Problems of Classical Elastostatics," Quarterly of Applied Mathematics, 25, 1967.

17. Swedlow, J.L. and Cruse, T.A., "Formulation of Boundary Integral Equations for Three-Dimensional Elasto-plastic Flow," International Journal of Solids and Structures, 7, 1971.

18. Thomson, W.T. and Kobori, T., "Dynamical Compliance of Rectangular Foundations on an Elastic Half-space," Journal of Applied Mechanics, ASME, 30, 1963.

19. Vardanega, C., "Soil-Structure Interaction Effects on the Dynamic Response of Shear Wall Buildings," M.Sc. Thesis, Dept. of Civil Engineering, M.I.T., June 1978.

20. Veletsos, A.S. and Wei, Y.T., "Lateral and Rocking Vibration of Footings," Journal of the Soil Mechanics and Foundations Division, ASCE, 97, 1971.

21. Werner, S.D., Lee, L.C., Wong, H.L. and Trifunac, M.D., "An Evaluation of the Effects of Traveling Seismic Waves on the Three-dimensional Response of Structures," Research Report R-7720-4514, Agbabian Associates, October, 1977.

22. Wong, H.L., "Dynamic Soil-structure Interaction," EERL-75-01, Ph.D. Thesis, California Institute of Technology, 1975.

23. Wong, H.L. and Luco, J.E., "Dynamic Response of Rigid Foundations of Arbitrary Shape," Earthquake Engineering and Structural Dynamics, 4, 1976.

24. Wong, H.L. and Luco, J.E., "Dynamic Response of Rectangular Foundations to Obliquely Incident Seismic Waves," Earthquake Engineering and Structural Dynamics, 6, 1978.